POLITECNICO
MILANO 1863

SCUOLA DI INGEGNERIA INDUSTRIALE
E DELL'INFORMAZIONE

Halogen-bonded complexes of N,N-Dimethylacrylamide with iodoperfluorocarbons

TESI DI LAUREA MAGISTRALE IN
MATERIALS ENGINEERING AND NANOTECHNOLOGY
INGEGNERIA DEI MATERIALI E DELLE NANOTECNOLOGIE

Author: **Edoardo Fiorani**

Student ID: 945872
Advisor: Pierangelo Metrangolo
Co-advisor: Gabriella Cavallo
Academic Year: 2021-22

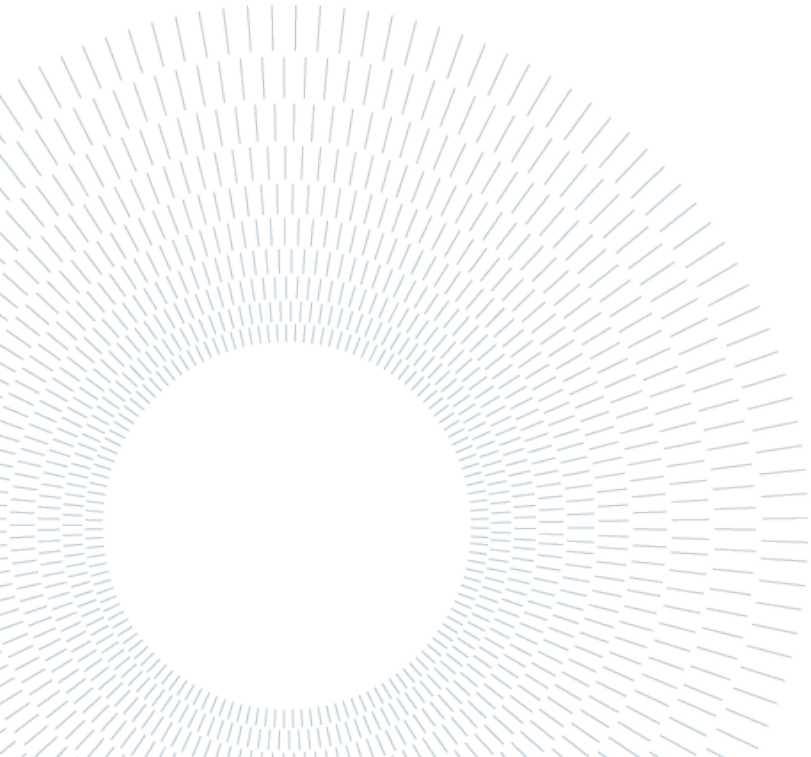

Abstract

The design of polymers capable of self-assembly has been the subject of intense study in the last decades, as it offers the possibility to obtain self-ordered structures with enhanced and new functionalities. Non-covalent interactions have proved to be an invaluable tool in the creation of these new materials. The halogen bond, thanks to its characteristic features like strength, directionality, and tunability, is gaining ever increasing interest in the development of novel supramolecular assemblies.

In this master thesis work halogen-bonded complexes of N,N-dimethylacrylamide with iodoperfluorocarbons have been prepared and characterized as a model system for poly(N,N-dimethylacrylamide) self-assembly. The formation of halogen bond has been confirmed with differential scanning calorimetry, infrared spectroscopy, and nuclear magnetic resonance spectroscopy. The results obtained on this model and the preliminary studies carried on poly(N,N-dimethylacrylamide) complexes shows that this polymer can be used to expand the possibilities in the design of halogen-bonded supramolecular materials.

Key-words: polymer self-assembly, halogen bond, N,N-dimethylacrylamide, poly(N,N-dimethylacrylamide, iodoperfluorocarbons.

Abstract in italiano

La necessità di ottenere materiali capaci di assumere strutture ordinate, con nuove e migliorate funzionalità per una grande varietà di applicazioni ha spinto la ricerca nell'ideazione di innovativi materiali polimerici capaci di auto-assemblarsi. Le interazioni non-covalenti si sono dimostrate uno strumento essenziale nella creazione di questi sistemi. Il legame alogeno, grazie alle sue peculiari caratteristiche come, direzionalità, capacità di regolarne la forza, e idrofobicità sta guadagnando sempre maggior interesse per lo sviluppo di nuovi sistemi sovramolecolari.

In questo lavoro di tesi magistrale complessi di N,N-dimetilacrilammide e iodoperfluorocarburi formati tramite legame alogeno sono stati preparati e caratterizzati, per avere un modello dell'auto-assemblaggio della poli(N,N-dimetilacrilammide). La formazione di legame alogeno è stata confermata tramite calorimetria differenziale a scansione, spettroscopia a infrarossi e spettroscopia a risonanza magnetica nucleare. I risultati ottenuti su questo modello e gli studi preliminari portati avanti su complessi di poli(N,N-dimetilacrilammide) dimostrano come questo polimero possa essere utilizzato per espandere le possibilità nella progettazione di materiali sovramolecolari con il legame alogeno.

Parole chiave: auto-assemblaggio di polimeri, legame alogeno, N,N-dimetilacrilammide, poli(N,N-dimetilacrilammide), iodoperfluorocarburi.

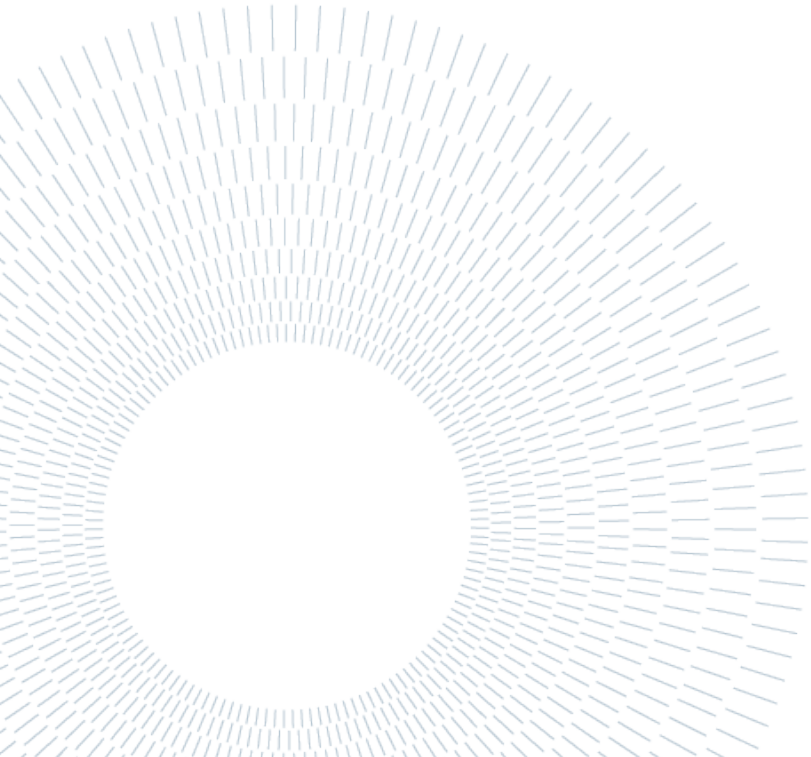

Contents

1 Introduction

1.1. Polymer Self-Assembly

The design of polymers capable of self-assembly has been the subject of intense research in the last decades, as it has been proved to be as a very effective strategy to obtain self-organized structures with new and enhanced functionalities. [1]

An established way to obtain self-assembled polymers has been the use of block copolymers, copolymers made by alternating blocks of different, immiscible, homopolymers that are covalently linked. Driven by the low affinity between the alternating blocks, these polymers have the ability to self-organize in distinct microphases rich in one of the different blocks, with domain sized of about 10-100 nanometers. Through careful adjustment of the molecular weight of the blocks, their volume fraction, and their mutual interactions, it is possible to obtain different structures, lamellar, cylindrical, spherical, and more complex shapes. [2],[3]

The self-assembly of block copolymers produces ordered nano-domains, but generally overall alignment at the macroscopic scale is missing, and a series of techniques have been devised to obtain long-scale ordering, required for certain potential applications like in microelectronic devices. Examples include the use of electric fields to orient the nanodomains parallel to the direction of the applied field, by taking advantage of the differences between the dielectric permittivity of the distinct segments; similarly magnetic field can be used thanks to the differences in

magnetic susceptibility. The application of shear forces is also an effective method to obtain long-scale order that does not require complex setups. Optical alignment using linear polarized light can be achieved with polymers that contains photoresponsive units like azobenzenes, that undergoes trans-to-cis isomerization upon illumination. Directed self-assembly techniques like graphoepitaxy and chemoepitaxy uses patterning of a substrate to direct the orientation of the nanostructures. [4]

Self-assembly properties have been successfully employed in a variety of applications. In nanolithography for example the possibility to obtain features sized in the range of 10-30 nm have attracted interest as it surpasses the limitations imposed by optical diffraction effects on traditional photolithography processes [5]. The possibility to selectively remove one of the blocks, leaving behind structures with specific textures, means that block copolymers can be used to fabricate nano-templates [6], [7]. In aqueous solution amphiphile block copolymers are capable to form vesicles with a wide variety of structures, with higher mechanical properties with respect to lipid-based ones and the possibility of tuning the permeability. Membranes that respond to environmental triggers for targeted delivery have been developed, and the research is focusing on how to exploit these structures in a variety of biomedical applications, like drug and gene delivery and synthetic nano-reactors. [8], [9]

A fundamental tool in the design of self-assembled materials is the use of non-covalent interactions. Taking advantage of the specificity, geometry, strength, and reversibility of these interactions, also called supramolecular interactions, it is possible to design highly functional and stimuli-sensitive materials, with the noteworthy advantage of avoiding complex processes of covalent chemical synthesis. Therefore, tuning the structure and the functionality of the building

modules it is possible to control at molecular level material structure, composition, morphology, and dimensions, enabling the construction of an extensive variety of structures. Non-covalent interactions are also sensitive to the environment, and the actual stoichiometry and structure of the self-assemblies can be influenced by the experimental conditions; design of materials based on non-covalent interactions needs to consider the complex and multiple bonding modes that can be present, and how to find a compromise might be necessary between strength of the interaction and the reversibility that might be desired by these systems [10]. Non-covalent interactions have been studied in biomedical applications, to obtain materials with new or enhanced electrical, magnetic, optical, self-healing properties and more, proving their invaluable use in material science. [10]–[12]

The use of non-covalent interactions plays an important role in driving polymer self-assembly. Polymeric materials obtained through non-covalent interactions are called supramolecular polymers. This name actually encompasses two main categories, main-chain supramolecular polymers, where the polymer backbone is held together by non-covalent interactions, and side-chain supramolecular polymers, consisting of a covalently linked polymer backbone containing specific molecular recognition units, to which specific sidechains can be non-covalently bonded. [11]

Concerning the second category of supramolecular polymers, the use of side-chains introduces a new level of self-assembly, with periodicity of a few nanometres, that combined with that of block copolymers, of about one order of magnitude bigger, can lead to structural hierarchies, as demonstrated by the simple model system of poly(styrene)-b-poly(4-vinylpyridine) with an hydrogen bonded amphiphile, where, by changing the relative length of the poly(4-vinylpyridine) block and the length of the amphiphile, formation of many different hierarchical structures,

lamellar-within-lamellar, lamellar-within-cylindrical, cylindrical-within-lamellar, spherical-within-lamellar, lamellar-within-spherical, was observed [13].

Supramolecular interactions have been used for instance to improve the performances of materials based on conjugated polymers. These polymers, that combine the semi-conducting characteristics of inorganic materials with the flexibility, processability and lower cost of polymers, have been used in photovoltaics, light-emitting diodes, and field-effect transistors. Since the electronic structure and the optoelectronic properties of these materials are dictated by their solid-state packing, the use of specific non-covalent interactions offers a relatively simple way to control the local packing arrangement. [14] Self-assembled hydrogen-bonded copolymers with temperature-dependant photonic bandgaps have been obtained both as liquid-crystals and films [15], [16]. The possibility to remove non-covalently bonded amphiphiles with selective solvent can alsobe exploited to obtain nanoporous membranes and nanotemplates [7], [17].

Along hydrogen bonding, π-π stacking, and other non-covalent interactions, halogen bonding, intensively studied in crystal engineering, has found increased interest for its potential use in the design of polymer self-assemblies [18], [19], and its peculiar features, which will be described in the next section, presents a host of possible advantages in many applications.

1.2. Halogen Bond

The halogen bond has an history dating back two centuries, but it was not until 2009 that IUPAC started a project to univocally define and classify the interactions involving halogen atoms as electrophilic species [18]. The project ended in 2013, with a recommendation that defined this interaction as follows: "A halogen bond occurs when there is evidence of a net attractive interaction between an electrophilic region associated with a halogen atom in a molecular entity and a nucleophilic region in another, or the same, molecular entity." [20]

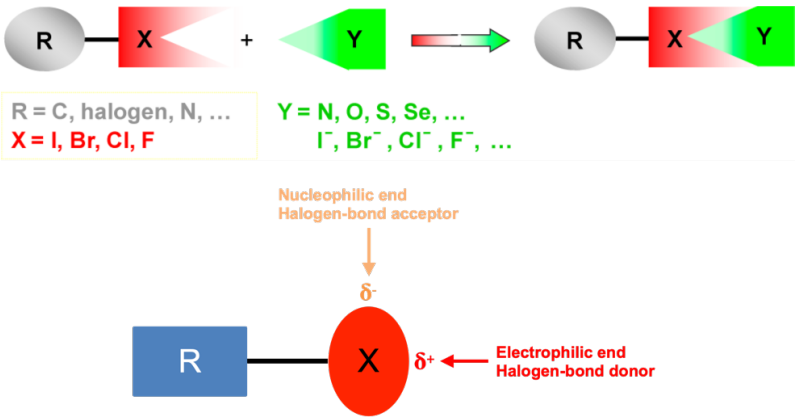

Figure 1.1: Schematic representation of the halogen bond. Highlighted are the electrophilic region, the σ-hole, and the nucleophilic region that arise from the anisotropic distribution of electron density.

This definition and the name halogen bond highlight the main features of this interaction, being that in involves a halogen atom, and that the role of the electron density acceptor, in analogy to the hydrogen bond, is played by said halogen atom.

The possibility to form a halogen bond arises from the fact that in covalently bonded halogen atoms the electron density has an anisotropic distribution, with the presence of a belt of negative electrostatic potential orthogonal to the covalent bond,

and a region of lower electron density, called σ-hole, focused along the elongation of the covalent bond, that can interact with nucleophilic species, resulting in highly directional interactions. [18]

Halogen bond (XB) presents some unique features that make it an unique tool in creating self-assembled systems: directionality, strength tunability, hydrophobicity and donor atom dimensions. [18], [21]

1.2.1. Directionality

The fact that the sigma-hole is localized on the elongation of the covalent bond the halogen atom is involved in leads to a strong directionality of the XB, with an angle between the covalent and noncovalent bond of approximately 180°. This strong directionality is maintained in species that can form more than one XB, for example in pyridine derivatives the C–X bond tend to be coplanar with the ring and the C–N··· X angles are approximately 120°.

1.2.2. Tunability

The strength of the halogen bond can be finely tuned by changing the halogen atom and the moiety covalently bonded to it. The positive character of the σ-hole increases with the polarizability, and decrease with the electronegativity, of the halogen atom, thus the XB donor ability increases in the order F < Cl < Br < I, as it can be seen in figure 1.2.

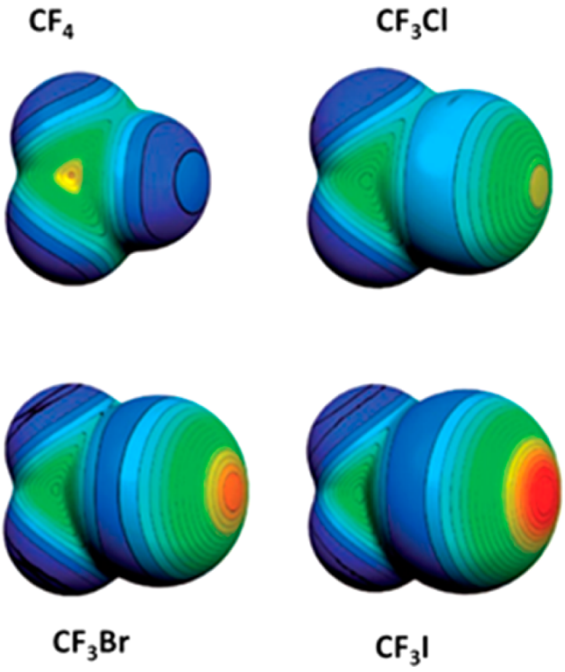

Figure 1.2: Electrostatic potential at isodensity surface for CF4, CF3Cl, CF3Br and CF3I. Color varies from blue for negative values and from green to red for increasing positive values [18].

The strength of the halogen bond is also influences by the electron-withdrawing nature of the atom or moiety covalently bound to the halogen atom. Strong electron-withdrawing moieties strengthen the sigma-hole, as was for example demonstrated by increasing the number of fluorine substituents onto a iodobenzene ring [22].

The characteristic of the XB acceptor also influence the strength of the bond. For example, nitrogen atoms tend to be better halogen bond acceptors than oxygen atoms, and anions are better acceptors than neutral species. [21]

1.2.3. Hydrophobicity

When halogen atoms are present in a molecule, they lead to an increase in its lipophilicity and hydrophobicity. Perfluorocarbons in particular do not mix well in aqueous or polar solvents, and it was shown that these solvents have little influence on the interaction energies and geometries of XB adducts. For this reason, halogen

bond can be seen as a hydrophobic equivalent of hydrogen bond, whose adducts instead suffer from the competition with solvents capable of HB. [18]

This behavior can be exploited to obtain for example halogen-bonded liquid crystals or in drug delivery applications, where various parameters like absorption, barrier permeability and interaction with the target molecules are influenced by the lipophilicity of the drug. [23]

1.2.4. Donor Atom Size

Halogen atoms have larger van der Waals radii with respect to the hydrogen atom, and this leads to some differences between the XB and the HB. For example, a downside of the bigger dimension of the atoms is that XB tends to be more sensitive to steric hindrance than HB.

The presence of larger atoms can instead be exploited in light-emitting materials, as the optoelectronic properties of supramolecular complexes can be influenced by the size of these atoms, that promotes singlet-to-triplet intersystem crossing through the heavy atom effect. [18]

1.2.5. Orthogonality between Hydrogen bond and halogen bond

Non-covalent interactions can be orthogonal, that is, they can drive self-assembly of the system without influencing each other, and they can be manipulated independently or simultaneously.

Hydrogen bond and halogen have been demonstrated to occur orthogonally not only on different acceptor sites [24], but also on the same site, as demonstrated in a study carried out on N-methylacetamide. The self-assembly of this molecule, chosen as it is the smallest one that mimics the peptide bond, was studied with various brominated and iodinated dihalotetrafluorobenzenes. The authors reported

that HB and XB occurred simultaneously on the carbonyl oxygen atom, and through x-ray diffraction it was observed that HB and XB were also geometrically orthogonal, with the values of the angle between them found in the range 77,9-98,5°. [25]

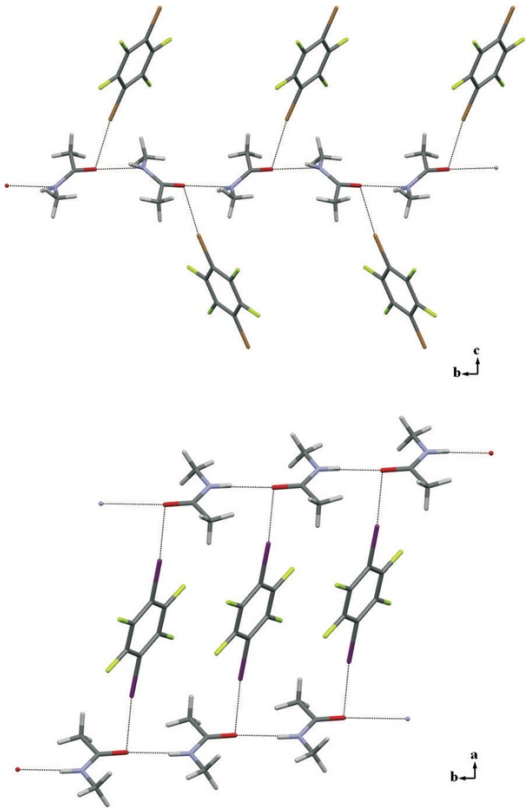

Figure 1.3: Simplified representation of the crystal packing of NMA chains via NH···O HB and interaction with 1,4-DITFB via I···O XB. [25]

1.3. Halogen Bond in Supramolecular Chemistry

1.3.1. Halogen Bond in Crystal Engineering

Crystal engineering is the understanding of intermolecular interactions in the context of crystal packing and the utilization of such understanding in design of new solids with desired physical and chemical properties [26]. Through numerous examples thoroughly collected in a review by NFMLab [18], it is possible to see how the directionality of halogen bonds has proved to be a powerful design element in this field, as it allows the supramolecular architecture to be more easily predicted from the structure of the starting compounds.

With the proper choice of starting molecules, a wide variety of supramolecular architectures have been obtained. One-dimensional chains can be obtained through self-assembly of self-complementary modules bearing both XB donor and acceptor sites or through self-assembly of ditopic XB donors and ditopic XB acceptors, and the arrangement of the chain is strictly related to the angle between the binding sites of the modules. Increasing the number of donor or acceptor sites it is possible to obtain two-dimensional architectures, like honeycomb structures. Using tetradentate modules three-dimensional systems have been achieved. Halogen-bonded two- and three-dimensional networks also frequently contain large potential cavities, and this, along with the strength and the high directionality of the interaction, have allowed to obtain robust and rigid supramolecular interpenetrated networks.

1.3.2. Halogen Bond in Material Science

Due to its properties, halogen bonding has also gradually gained interest in various fields of material science, including soft materials like liquid crystals, gels, and polymers.

The use of fluorinated groups is an efficient strategy to improve the properties of liquid crystals and control their supramolecular organization, and halogen bonding with haloperfluorocarbons has been successfully used to obtain supramolecular liquid crystals starting from non-mesomorphic components, as was first reported in complexes with alkoxystilbazoles as XB acceptors and iodopentafluorobenzene as XB donor [27]. Low molecular weight liquid crystals were also obtained with alkoxystilbazoles and α,ω-diiodoperfluoroalkanes as bidentate halogen bond donors; interestingly, while usually the presence of long fluoroalkyl chains drive segregation into lamellar smectic A phases, precluding the appearance of nematic phases, the liquid crystals obtained all showed monotropic nematic phases. [28]

Gel-phase materials are of particular interest in regenerative medicine, tissue engineering and drug delivery, and research has focused on how to apply molecular recognition processes to control the strength of the gel and the gelation process through noncovalent interactions, starting from simple molecules. [29] It was demonstrated that halogen bonding can be used to promote the gelation process, as first shown with various bis(urea) compounds that in normal condition are non-gelators in aqueous and polar solvents; supramolecular gelation was instead induced through the formation of XB. [30]

Taking advantage from the modularity of the bottom-up approach enabled by halogen bond, many functional systems have been obtained. In the design of light-emitting materials, where the electric and optic properties of chromophores are

defined also by the intermolecular electronic packing, and so by their packing in the solid state [31], the use of halogenation and XB seems an interesting perspective, as first demonstrated in studies on a stilbene derivative co-crystallized with various non-fluorescent XB donors; the different crystal packings resulted in different optical properties, with emission colours ranging from blue to green and yellow [32]. The already mentioned heavy-atom effect can be exploited to increase the rate of singlet-to-triplet intersystem crossing, a feature particularly useful in the design of phosphorescent materials. [18] XB have also been used in the design of light-responsive materials containing azobenzene. A study on a halogen-bonded system of azobenzene and stilbazole found that spin-casted films of the complex are capable of efficient photoalignment, with a high surface relief grating formation efficiency that led to a depth modulation 2,4 times the initial thickness. These results could be partly attributed to the presence of an high temperature nematic phase, enabled by XB. [33]

1.4. Halogen Bond in Polymer Science

Although crystal engineering has been the principal area of research of halogen bonding, the concepts and knowledge acquired in that field have also been extended to the study of self-assembled polymers.

As already seen with liquid crystals and gels, the structural organization of soft materials is greatly influenced by the nature of the intermolecular interactions formed and the halogen bond, due to its strength and geometrical features, can be a powerful tool to obtain polymeric materials with complex structures and new functionalities.

1.4.1. Polymer Self-Assembly

The first report of a halogen bond-driven supramolecular polymer was that of a poly(4-vinylpyridine)/diiodoperfluoroalkane supramolecular comb-shaped polymer. In the study the formation of a comb-like structure due to segregation of the perfluorocarbon chains in fluorinated layers with smectic arrangement alternating with hydrocarbon layers was observed. The authors highlighted that the high directionality of XB, the rigid rod-like structure of the perfluorocarbon and their tendency to segregate can contribute to liquid crystalline properties of these materials. [34]

As explained in the first paragraph, a strategy commonly used to obtain polymeric hierarchical structures is to use block copolymers. The low affinity of dissimilar blocks lead to microphase separation, and this tendency can be promoted by complexation of one of the blocks with low molecular weight additives. Halogen bond has thus been used to obtain a lamellae-within-cylinder structure with a poly(styrene)-block-poly(4-vinylpyridine) di-block copolymer, using 1,8-

diiodoperfluorooctane (DIPFO) as additive. Cylindrical phases arranged mainly in a hexagonal pattern, and in spin coated films it was found that upright cylindrical alignment could be achieved spontaneously, without the need for external stimuli. The authors suggested that this upright alignment was due to the low surface energy of diiodoperfluorooctane. Removal of DIPFO using ethanol also showed that the film was able to retain its structure. [35]

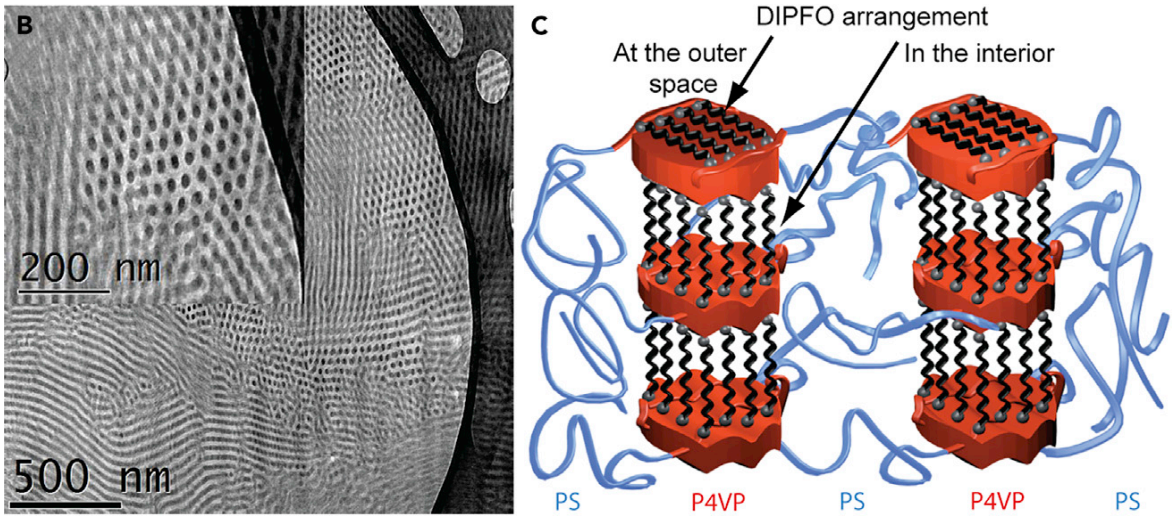

Figure 1.4: TEM micrograph of the PS-b-P4VP(DIPFO) bulk sample and schematic representation of the lamellae-within-cylinder structure [35]

Moreover, self-assembled polymeric structures generally present only local order, and to obtain alignment at the bulk scale different techniques have been employed, like the application of electric, magnetic or flow fields, surface templating and thermal or solvent annealing [4]. Through halogen bonding it was possible to achieve alignment up to the millimeter scale without external stimuli of an amine hydrochloride derivative of a 4-arm polyethylene glycol with 1-iodoperfluorodecane and 1-iodoperfluorododecane, with the halogen bonds occurring between the chlorine anions and the iodine atoms. This result was due to the strength and directionality of the XB, together with the tendency of the perfluoroalkyl chains to segregate in straight interfaces. [36]

Self-assembly of polymers through halogen bonding has been achieved not only through the addition of perfluorocarbons, but also through the functionalization of polymers with halogen bond donor groups. For example, a layer-by-layer assembly of poly(4-(4-iodo-2,3,5,6-tetrafluorophenoxy)-butyl acrylate) (PIPBA) and poly(vinylpyiridine) obtained. Upon observation that the hydrogen bonded equivalent using poly(4-vinylphenole) (PVPy) of the film was more stable, and since PVPy is also capable of forming XB, the authors prepared a hybrid structure which alternate also (PIPBA/PVPy/PVPh/PVPy)5, and the hybrid film proved to be much more stable than the one with only XB. [37]

The possibility of self-assembly in solution-phase through halogen bonding has also been demonstrated. In the first study on the subject the authors synthetized a block copolymer of poly(ethyleneoxide) and poly(2-dimethylamino ethylmethacrylate) (PEO-b-PDMAEMA), with the PDMAEMA containing the XB acceptor sites, and a iodotetrafluorophenoxy substituted polymethacrylate as hydrogen bond donor. The two polymers were dissolved in DMSO, and upon addition of water and dialysis wormlike structure due to aggregation of individual spherical particles were observed. The experiments were also repeated with organic solvents, and self-assembled structures were also observed, although without the structure obtained in water. [38]

1.4.2. Solid-Phase Polymerization

Solid-phase polymerization (SPP), also called solid-state polymerization, is a technique used to polymerise solid monomers and monomer crystals/co-crystals, able to yield polymers with high molecular weights. SPP presents also the advantage that it can proceed under topochemical control, resulting in high regio- and stereoselectivity, and it can be performed in a solvent-free environment. [39]

Recently solid phase polymerization was performed on a series of co-crystals of vinyl monomers (4-vinylpyridine, 2-vinylpyridine, 2-vinylpyrazine, 1-vinylimidazole, N-vinylpyrrolidone and N,N-dimethylacrylamide) as XB acceptors, and 1,4-diiodotetrafluorobenzene as XB donor. Once obtained, polymerization of the co-crystals was performed using a thermal initiator or a photoinitiator. In both cases solid phase polymerization led to high monomer conversions, higher molecular weight, and lower polydispersity with respect to the solution polymerizations. The authors also fabricated more complex structures using mixtures of N-vinylpyrridone or N,N-dimethylacrylamide, ethylene glycol dimethylacrylate as cross-linkable co-monomer, 1,4-diiodotetrafluorobenzene, and 2,2-dimethoxy-2-phenyl-aceto-phenone as photoinitiator. Monomer sheets of the two different monomers were prepared, pasted together and UV-irradiated. After polymerization ethanol was used to remove the diiodotetrafluorobenzene, and shape retention showed that crosslinking was successful. [40]

1.4.3. Light-Responsive Supramolecular Polymers

As described previously, efficient light-induced surface patterning was obtained with azeobenzene-stilbazole halogen-bonded complexes. [33] The same principles have been applied in designing high-performance supramolecular polymers for light-induced surface patterning. Poly(4-vinylpyridine) has been used as halogen bond acceptor, while different azobenzene derivatives have been used, to study the effect of single atom mutation on the complex. Solutions of the polymer-dye mixtures were dissolved in dimethyl formamide, and thin films were spin-casted onto a substrate. The authors demonstrated that the grating formation efficiency can be related to the strength and the nature of the non-covalent interaction, and that the higher directionality of the halogen bond enhances the mass transport

phenomena. The possibility of tuning the bond strength by single atom mutation can also offer a useful tool in the study of surface relief grating formation. [41]

1.4.4. Self-Healing

Intrinsic self-healing polymers possess the ability to repair molecular and macroscale damage through a temporarily increase of local mobility of the polymer chains. Supramolecular interactions, due to their reversible nature, seems then ideal to create self-healing polymers. [42] The first reported example of self-healing polymers based on halogen bond involved two functionalized polymers based on butyl methacrylate, one containing a halogen bond donor group, the other containing a halogen bond acceptor group. The ability to undergoing self-healing multiple times was demonstrated through scratch-healing tests, with recovery at 100°C. [43]

1.5. Master Thesis Project Overview

From the previous sections some of the strategies more commonly used in the design of halogen-bonded polymer systems have emerged. For example, poly(4-vinylpyridine) has been frequently employed, both alone and in block copolymers, due to presence of the pyridine ring, an effective XB acceptor group; 1,4-diiodotetrafluorobenzene is commonly used as XB donor, as are long perfluoroalkyl chains, thanks to their strong tendency to segregate.

Poly(N,N-dimethylacrylamide) (PDMA) is an hydrophilic biocompatible polymer, that has been studied in applications like DNA sequencing and drug delivery systems [44], [45]. In a 2013 article PDMA has been used successfully in a block copolymer with poly(4-vinylpyridine), to obtain a double comb-like system through the addition of 3-pentadecylphenol, that was able to form hydrogen bond with both the nitrogen of the pyridine ring and the oxygen of the carbonyl. This has led to a lamellar-in-lamellar structure, with a large length scale given by the phase separation between the different supramolecular blocks, and both domains then showed a smaller lamellar morphology, perpendicular to the large length structure, with different periodicity due to the difference in the supramolecular interactions. [46]

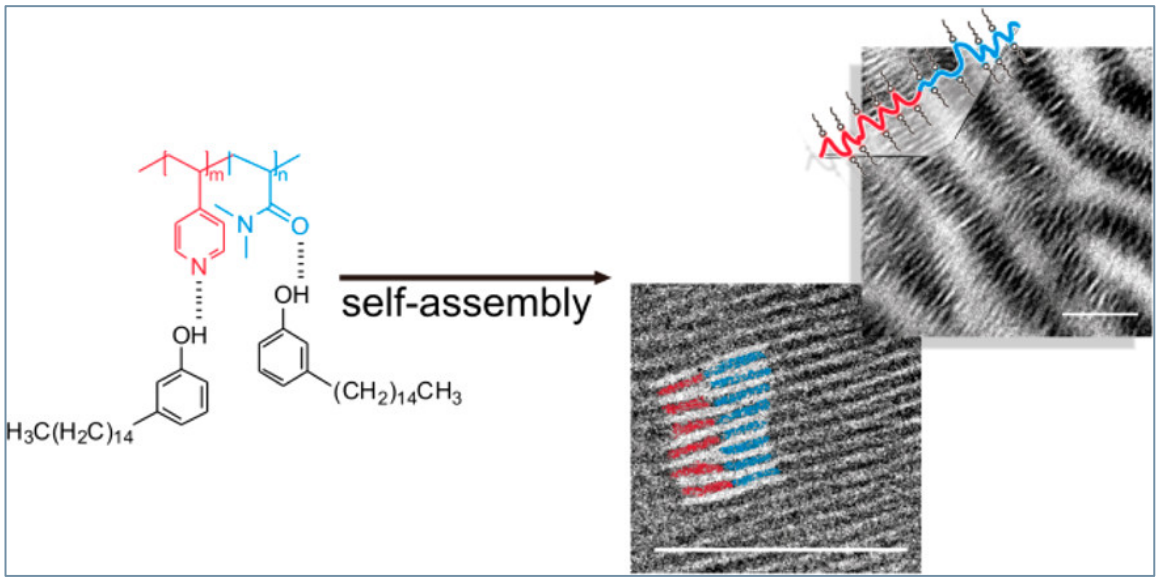

Figure 1.5: Schematic representation and TEM images of the P4VP-b-PDMA(PDP) supramolecular complex. [46]

While poly(4-vinylpyridine) has been extensively used [24, 25, 27], poly(N,N-dimethylacrylamide) has not yet been reported as being used in halogen-bonded supramolecular systems [19]. Its monomer N,N-dimethylacrylamide has been used in solid-phase polymerization of halogen bonded co-crystals with 1,4-diiodotetrafluorobenzene, as already mentioned [40]. Due to the analogies between hydrogen bond and halogen bond it is expected that PDMA could also self-assemble with halogen bond donors. If this hypothesis is proved correct it will lead to a new addition to the list of polymers that can be used to design halogen-bonded supramolecular polymer self-assemblies.

In this master thesis work the main focus has been the characterization of the supramolecular interaction of the monomer N,N-dimethylacrylamide with various iodoperfluorocarbons, to obtain a model system for the self-assembly of the polymer. Corresponding systems using hydrogen bond donors have been characterised to compare the two interactions. Studies have also been made on the possibility to obtain ternary co-crystals between N,N-dimethylacrylamide and both an halogen and an hydrogen bond donor. Finally, along the studies on the model

system, preliminary experiments on poly(N,N-dimethylacrylamide) halogen-bonded complexes have also been performed.

2 Materials and Methods

2.1. Materials and Solvents

The halogen-bonded complexes were prepared with both the monomer and the corresponding polymer: N,N-Dimethylacrylamide – 99%, contains 500 ppm monomethyl ether hydroquinone as inhibitor – Sigma-Aldrich; Poly(N,N-dimethylacrylamide), DDMAT terminated - Average M_n 10,000, PDI ≤1.1 – Sigma-Aldrich.

The following molecules were used as halogen bond donors: Perfluorohexyl Iodide 98% (Apollo Scientific); Heptadecafluoro-1-Iodooctane (Fluka Analytical); Perfluorodecyl Iodide (Apollo Scientific); Perfluorododecyl Iodide (Apollo Scientific); 1,4-Diiodoperfluorobenzene (Apollo Scientific); 1,2-Diiodotetrafluoroethane (Apollo Scientific); 1,4-Diiodooctafluorobutane (Apollo Scientific); 1,6-Diiodododecafluorohexane (Apollo Scientific); 1,8-Diiodoperfluorooctane (Apollo Scientific); Iodopentafluorobenzene (Fluorochem).

The following molecules were used as hydrogen bond donors:

Ethylene Glycol (Fluka); Phenol (Sigma-Aldrich); Hydroquinone (Carlo Erba Reagents).

In the preparation and the analysis of the complexes the following solvents were used: Chloroform (Carlo Erba Reagents); Dichloromethane (Carlo Erba Reagents); Acetone (Carlo Erba Reagents); Acetonitrile (Carlo Erba Reagents);

Tetrahydrofuran (Fisher Chemical); Chloroform-d – 99.8 atom % D – Sigma Aldrich; n-Pentane, 98% (abcr); 2,2,2-Trifluoroethanol - analytical standard, for NMR spectroscopy (Sigma Aldrich); Trifluoroacetic acid for synthesis (Sigma Aldrich); Deuterium oxide 99.9 atom % D (Sigma Aldrich).

All the chemicals have been used without further purification.

2.2. Preparation of N,N-Dimethylacrylamide Binary Samples

N,N-dimethylacrylamide (DMA) has been chosen as model compound for poly(N,N-dimethylacrylamide) (PDMA). Its ability to act as a halogen bond acceptor has been first evaluated by preparing binary mixtures with various iodoperfluorocarbons.

Since the oxygen of the carbonyl can form one or two halogen bonds [47], [48], to determine the binding mode with halogen bond donors samples have been prepared at different ratios between the DMA and XB donor, with 1 or 2 equivalent of iodine atoms per carbonyl group.

For the ditopic halogen bond donors, α,ω-diiodoperfluoroalkanes (DIPFn n = number of C atom in the molecule = 2, 4, 6, 8) and 1,4-diiodotetrafluorobenzene (DITFB) were chosen, and the hypothesis was made that both iodine atoms of the molecules form XB; samples were prepared at two stoichiometric ratios between DMA and the XB donor: 2 : 1 for the hypothesis of monodentate oxygen, and 1 : 1 for the hypothesis of bidentate oxygen.

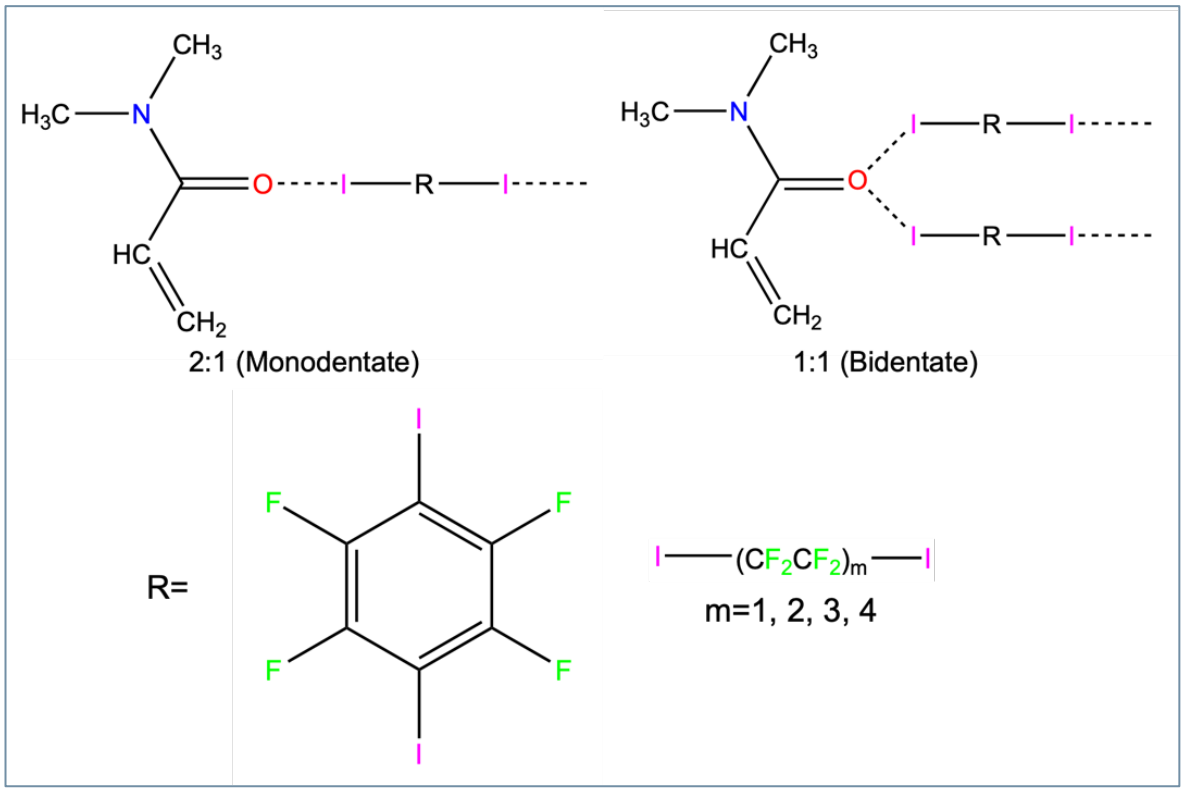

Figure 2.1: Scheme of the DMA complexes with ditopic XB donors.

For the monotopic halogen bond donors, 1-iodoperfluoroalkanes (IPFn n = number of C atom in the molecule = 6, 8, 10) and iodopentafluorobenzene (IPFB), were used. Samples were again prepared at two stoichiometric ratios between DMA and the XB donor: 1 : 1 for the hypothesis of monodentate oxygen and 1 : 2 for the hypothesis of bidentate oxygen.

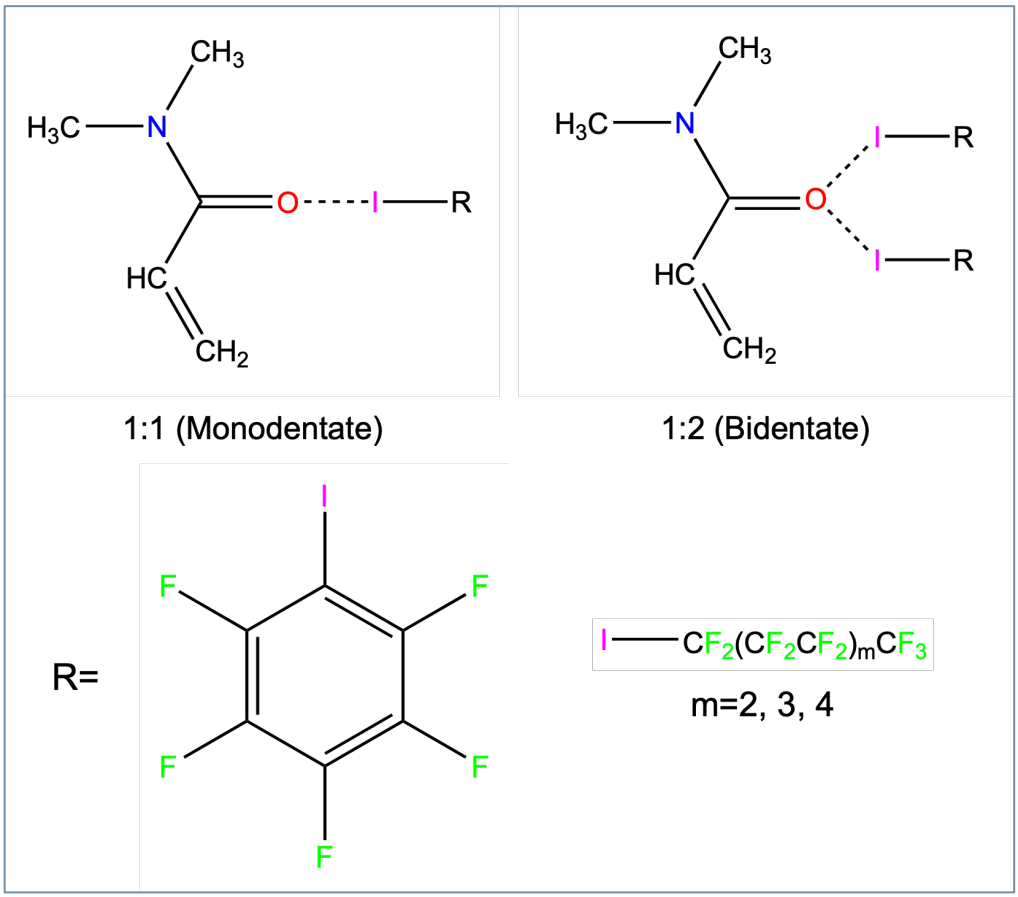

Figure 2.2: Scheme of the DMA complexes with monotopic XB donors.

DMA is liquid at room temperature, and it can act as solvent with 1-iodoperfluorohexane (IPF6), 1-iodoperfluorooctane (IPFO), 1,2-diiodoperfluoroethane (DIPF2), 1,4-diiodoperfluorobutane (DIPF4), 1,6-diiodoperfluorohexane (DIPF6), and iodopentafluorobenzene (IPFB), which are also liquid at room temperature, and 1,8-diiodoperfluorooctane (DIPFO), solid at room temperature. In the preparation of the complexes with these XB donors the two components have simply been mixed, without the use of any additional solvent. The mixtures were then left overnight and analysed.

DMA was instead not able to dissolve 1,4-diiodotetrafluorobenzene (DITFB) and 1-iodoperfluorodecane (IPF10), and their preparation required the use of chloroform. Two different crystallization methods were used to obtain their complexes, both

carried out by isothermal evaporation of the solvent at room temperature. The first was called fast solvent evaporation: the XB donor was dissolved in chloroform, and DMA was added to the solution. The vial with the mixture was covered with parafilm, some holes were made in the parafilm, and the vial was left under hood for solvent evaporation. In the second one, called slow solvent evaporation, the XB donor was dissolved in chloroform using the minimum quantity of solvent necessary, and DMA was added to the solution. The vial with the mixture was then put in jars containing paraffin oil for the solvent evaporation, to carry the crystallization process in a controlled atmosphere saturated with solvent vapours.

Slow solvent evaporation was also performed on solutions of N,N-dimethylacrylamide/1,4-diodotetraflurobenzene using different solvents instead of chloroform: dichloromethane, acetone, acetonitrile and tetrahydrofuran.

The behaviour of DMA with the corresponding hydrogen bond donors of some of the XB donors used was also studied, to understand what differences another non-covalent have on the self-assembly. Three HB donors were used: phenol (PH) as the counterpart of iodopentafluorobenzene, hydroquinone (HQ) as counterpart of 1,4-diiodotetrafluorbenzene, and ethylene glycol (EG) as counterpart of 1,2-diiodoperfluoroethane. The samples were prepared only considering a 1 : 1 ratio between OH and CO groups. Ethylene glycol was mixed directly with DMA, while for phenol and hydroquinone the slow solvent evaporation procedure was followed.

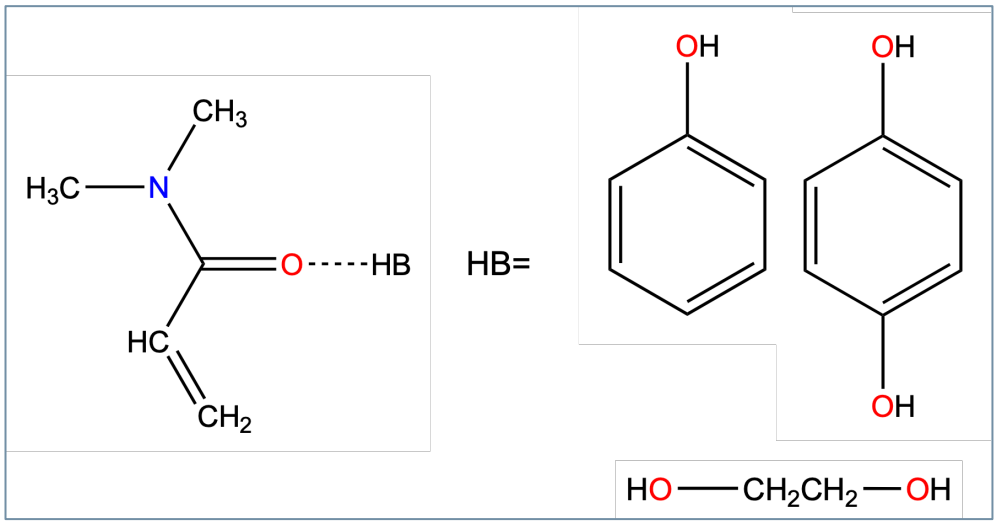

Figure 2.3: Scheme of the DMA complexes with HB donors.

2.3. Preparation of N,N-Dimethylacrylamide Ternary Samples

As seen in the introduction a study on a model system of N-methylacetamide with DITFB has shown that orthogonal XB and HB can form on the carbonyl atom, and it was reasoned that it was worth to explore this possibility also in the system with DMA. Ternary solutions with N,N-dimethylacrylamide and one halogen bond donor and one hydrogen bond donor were also prepared.

Three samples were made, using an XB donor and its corresponding HB donor: the first was N,N-dimethylacrylamide/ethylene glycol/1,2-diiodoperfluoroethane (DMA/EG/DIPF2), prepared mixing directly the three liquid components; N,N-dimethylacrylamide/phenol/iodopentafluorobenzene (DMA/PH/IPFB) and N,N-dimethylacrylamide/hydroquinone/1,4-diiodotetrafluorobenzene (DMA/HQ/DITFB), were instead prepared with the slow solvent evaporation procedure.

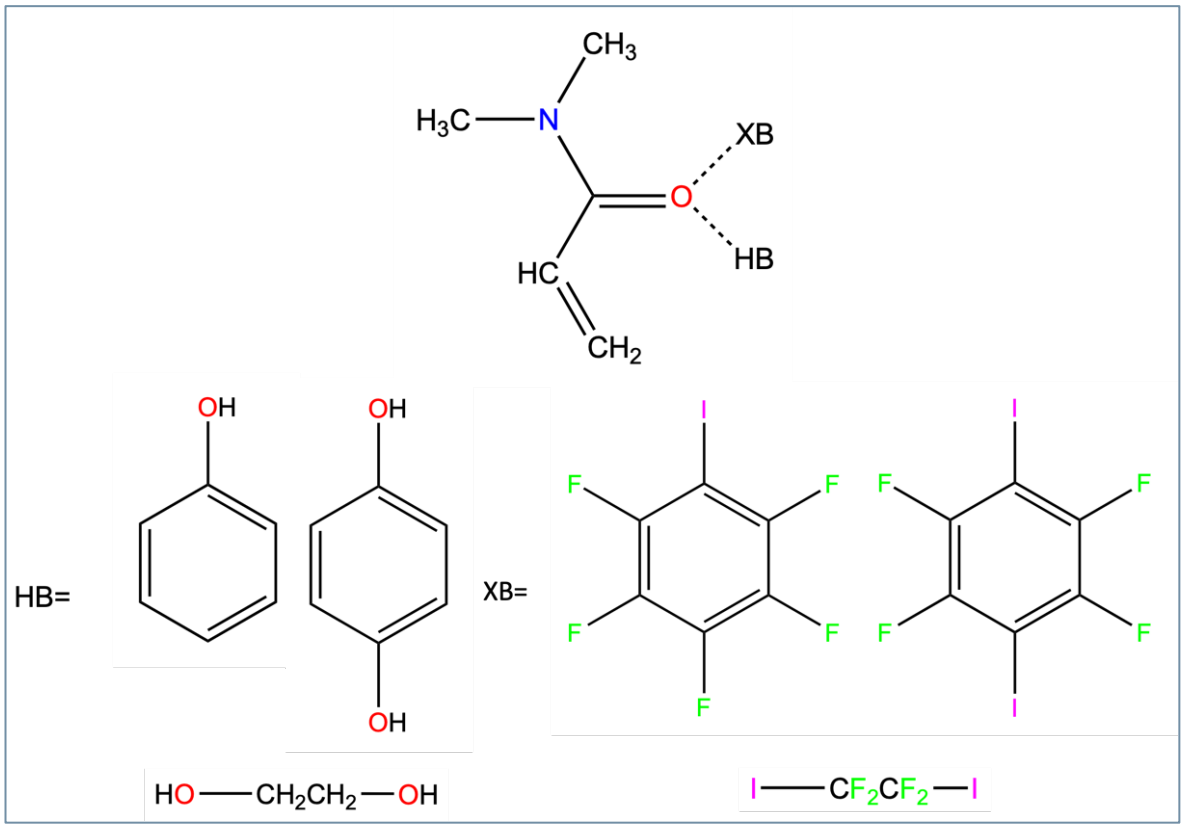

Figure 2.4: Scheme of the DMA ternary complexes.

2.4. Preparation of Poly(N,N-dimethylacrylamide) Samples

Along the study of the model with the monomer, preliminary attempts to obtain co-crystals of poly(N,N-dimethylacrylamide) with various XB donors have been made.

All the samples prepared with poly(N,N-dimethylacrylamide) were made considering a 1 : 1 ratio between carbonyl groups and iodine atoms; given the molecular weight of the polymer (M_n=10.000) approximately 100 carbonyl groups are present on each chain, and thus the corresponding quantity of XB donor has been used. Different procedures were explored for the synthesis of these complexes.

The first method used was slow isothermal evaporation of the solvent at room temperature. With this method samples were prepared with 1-iodoperfluorohexane (IPF6), 1-iodoperfluorodecane (IPF10) and 1-iodoperfluorododecane (IPF12). PDMA and the XB donor were dissolved separately in chloroform, and the solutions were then mixed. The mixture was stirred for 24 hours, then the vials containing the solution were put into jars containing chloroform to achieve crystallization in an atmosphere saturated with vapours of the solvent. The crystallization was carried out for approximately three weeks, after which the vials were removed from the jars, the samples dried completely under hood and then analysed.

The second procedure was fast isothermal evaporation of the solvent under hood, a faster process in non-controlled atmosphere. Samples were prepared with a wider range of halogen bond donors: 1-iodoperfluorohexane (IPF6), 1-iodoperfluorooctane (IPF8), 1-iodoperfluorodecane (IPF10), 1,8-diiodoperfluorooctane (DIPF8) and 1,4-diiodotetrafluorobenzene (DITFB). A sample was also prepared with 3-pentadecylphenol (PDP) to have a comparison

with the hydrogen bonded complex seen in the article by Faber et al. [46]. PDMA and the XB donor/PDP were dissolved separately in chloroform, and the solutions were then mixed. The mixture was stirred for 2h, then the vial with the solution was covered with parafilm, in which holes were made using a needle, and left under hood for solvent evaporation.

The third procedure used was melting. Due to the high temperatures of this method and the volatility of shorter iodoperfluoroalkanes, samples were prepared using 1-iodoperfluorodecane (IPF10), 1-iodoperfluorododecane (IPF12) and 1,4-diiodotetrafluorobenzene (DITFB). PDMA and the XB donor were put together in a vial and mixed with a spatula. The mix was than heated at 200°C, the melting temperature of the polymer, and kept at this temperature for 5 min. After cooling the mixture was mixed again with a spatula, and the process was repeated 5 times.

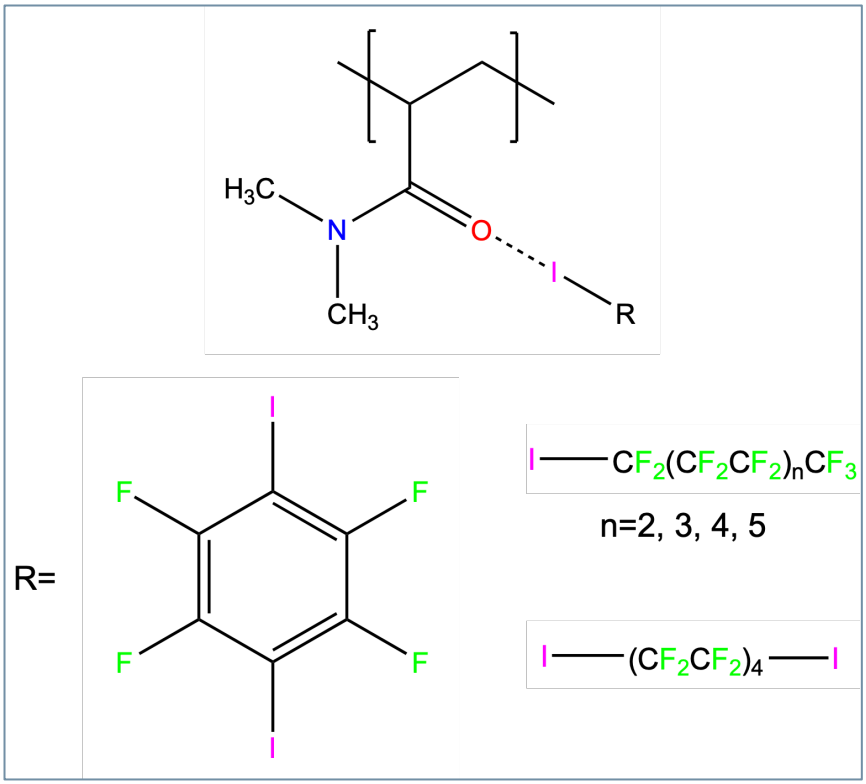

Figure 2.5: Scheme of the PDMA complexes prepared with XB donors.

2.5. Differential Scanning Calorimetry

Differential scanning calorimetry (DSC) is a fundamental technique in thermal analysis. It is based on the measure of the difference in heat flow rate against temperature between the sample and a reference during a controlled temperature program. It can be used to measure the characteristic temperatures of the sample, like melting and crystallization temperatures, and secondary transitions like glass transition, heat capacity of the material and so on. Since heat flow can't be measured directly, it is actually the difference in temperature between the sample and a reference that is actually used to calculate the heat flow. [49]

DSC was utilized to assess the formation of a complex between DMA and the various halogen bond donors through the presence of melting and crystallization peaks not ascribable to the monomer nor the XB donor, and to determine the stoichiometry of said complex through the absence or the eventual presence of the peaks of the starting compounds.

DSC analyses were performed on a METTLER TOLEDO DSC823^{e} module, using 40ul aluminium pans for the sample and the reference. The results were evaluated using the STAR^{e} software 12.

2.6. Infrared Spectroscopy

Infrared (IR) spectroscopy is a fundamental tool in chemical spectroscopy, and the observation of vibration shifts can be very useful to establish the formation of XB. It is a vibrational spectroscopy, as IR absorption in molecules is associated with various kind of vibrations, which can be due to changes in bond length or in bond angle. An IR spectrum can be divided in two regions: the group frequency region between about 3600 and 1250 cm-1, through which is possible to identify what functional groups are present in a molecule, and the fingerprint region between 1250 and 600 cm-1, where small differences in the molecule structure are associated with significant changes in the absorption behaviour, and so can be used to easily identify a known molecule. [50]

2.6.1. ATR Infrared Spectroscopy

Attenuated total reflectance (ATR) - IR spectroscopy is a technique that can be used to acquire IR spectra with a wide variety of samples and almost no preparation and it is based on the phenomenon of total internal reflection.

In ATR-IR the infrared light is shone on a transparent crystalline material with high refractive index in condition of total internal reflection; the sample is placed above this material, and the radiation is reflected, and thus partially absorbed, multiple times before reaching the detector. The spectra obtained are similar to those obtained through classic IR-spectroscopy. [50]

To characterize XB formation IR spectroscopy is used to monitor the stretching modes of the C—F bond in the 1200-1000 cm-1 region and the shift of the C—I bond in the far region, and concerning DMA, iodine coordination with the oxygen of a

carbonyl bond can be detected through a red-shift of the C=O stretching peak and a blue-shift of the C—N stretching signal [9].

ATR-IR analyses were performed using a VARIAN 640-IR, and the results were evaluated using the Omnic 8.3 software.

2.7. Nuclear Magnetic Resonance Spectroscopy

Nuclear magnetic resonance (NMR) spectroscopy is one of the techniques of choice in investigating XB. Certain atoms with non-zero spin, like 1H, 13C, 19F and 31P, possess a magnetic moment oriented alongside the axis of spin; when the nucleus is brought into an external magnetic field, its magnetic moment becomes orientated in different directions depending on its quantum state. The potential energy of a nucleus is proportional to the external magnetic field and related to its quantum state, thus the application of an external field causes a splitting in the energy levels of the nucleus. Transition between energy states can then happen by absorption or emission of electromagnetic radiation with a frequency corresponding to that energy gap.

The frequency of the radiation absorbed by a certain nucleus is affected by its chemical environment, an effect called chemical shift. The chemical shift is due to the fact that the electrons that circulate around a nucleus create a small magnetic field, that opposes the applied one; the internal field is proportional to the applied field and to a screening constant, that is determined by the electron density and its distribution around the nucleus: the more a nucleus is shielded, the stronger the field that needs to be applied or the frequency of the oscillator. Chemical-shift resonances also present a superimposed effect called spin-spin splitting, that is due to interaction of a nucleus with the magnetic moments of adjacent ones; the multiplicity, that is the number of split peaks observed for a nucleus, depends on the number of non-equivalent nuclei adjacent to it. This effect is also independent of the applied field, so it can be easily distinguished form the chemical-shift by changing the applied field. [50]

19F NMR is particularly useful to study the formation of XB, due to the high sensitivity and wide chemical shift range of this nucleus. With iodoperfluorocarbons, a shift up-field of the signal of the fluorine atoms next to iodine is an indication of the formation of the bond. [18]

2.7.1. NMR Spectroscopy of Solid Halogen-bonded DMA Complexes

The solid binary complexes of DMA, that are N,N-dimethylacrylamide/1-Iodoperfluorodecane and N,N-dimethylacrylamide/1,4-diiodotetrafluorobenzene, have been prepared by diluting 10 mg of the sample in 0,5 ml of deuterated chloroform. As internal reference a solution containing 100 µl of 2,2,2-Trifluoroethanol in 1 ml of deuterated chloroform was prepared, and 10 µl were added to the solution in the tube; this reference was used both to fix the values of the 19F spectra and to determine the stoichiometry of the samples. The spectra of the pure starting compounds were collected by maintaining the concentration of DMA and XB donor in chloroform-d the same as for the complexes, to partially offset the effect of the concentration on the chemical shifts.

2.7.2. NMR Spectroscopy of Liquid Halogen-bonded DMA Complexes

Regarding the liquid samples, to prove that the intermolecular interaction was occurs and to have a first indication of its strength, 19F spectra were collected using pure samples in a coaxial tube, with an external reference made of trifluoroacetic acid diluted in deuterium oxide at a concentration of $5{,}54\times10^{-3}$ mol/ml. Reference spectra were collected by diluting the XB donors in n-pentane at the same concentration as in the complex.

NMR spectroscopy was performed on a Bruker AV400 spectrometer. Data evaluation was done with the MestreNova 10.0 software.

2.8. Thermogravimetric Analysis

Thermogravimetric analysis (TGA) is a technique through which the mass of a sample is monitored during a temperature program that can consist of different temperature ramps and isothermal holds.

A thermogravimetric analyzer consists in a precise balance connected to a sample pan. The sample pan is inside a furnace, were the temperature is monitored through a thermocouple and a dynamic purge gas is passed over the sample to remove gases and volatile compounds that are liberated during the process. [51]

TGA was performed on some of the PDMA binary and ternary complexes, to monitor differences in the thermogram with respect to the pure compounds, that can be an indication on the formation of an intermolecular interaction.

TGA were performed on a TA Instruments TGA Q500, using a linear heating ramp from room temperature up to 500°C at 5°C/min, and data evaluation was made using the Universal Analysis 2000 software.

3 Results

3.1. N,N-Dimethylacrylamide Binary Samples

The samples DMA/DIPF2, DMA/DIPF4, DMA/DIPF6, DMA/DIPF8, DMA/IPF6, DMA/IPF8 and DMA/IPFB, prepared without additional solvent, didn't form any precipitate, (figures 3.2 and 3.3), and DSC confirmed that the melting point of these complexes is below room temperature.

Crystallization carried on the N,N-dimethylacrylamide/1-iodoperfluorodecane solutions with the two solvent evaporation processes gave similar results with the fast and the slow sone. In both cases a white, slightly sticky powder was obtained.

Crystallization carried on N,N-dimethylacrylamide/1,4-diiodotetrafluorobenzene solutions also gave similar results with the two procedures. In the case of the fast process small, elongated crystals were obtained. With the slow process better crystals were obtained, around 1-2 mm long. (Figure 3.1) Regarding the crystallizations carried out with other solvents, dichloromethane gave similar results as chloroform, while with acetone, acetonitrile and tetrahydrofuran only powdery deposits formed; through IR spectroscopy it was observed that the shifts of the C=O were 1-2 cm^{-1} smaller in the samples prepared with acetone, acetonitrile and tetrahydrofuran, and no other difference could be observed in the spectra.

All three samples with hydrogen bond donors showed no formation of precipitate. Though prepared with the slow solvent evaporation, DMA/PH and DMA/HQ were liquid at room temperature, and the latter solution also assumed a strong red

coloration; proton NMR was performed on this sample, but the presence of all the peaks of the starting compounds suggest that the coloration is not due to a chemical reaction but due to the formation of the non-covalent interaction.

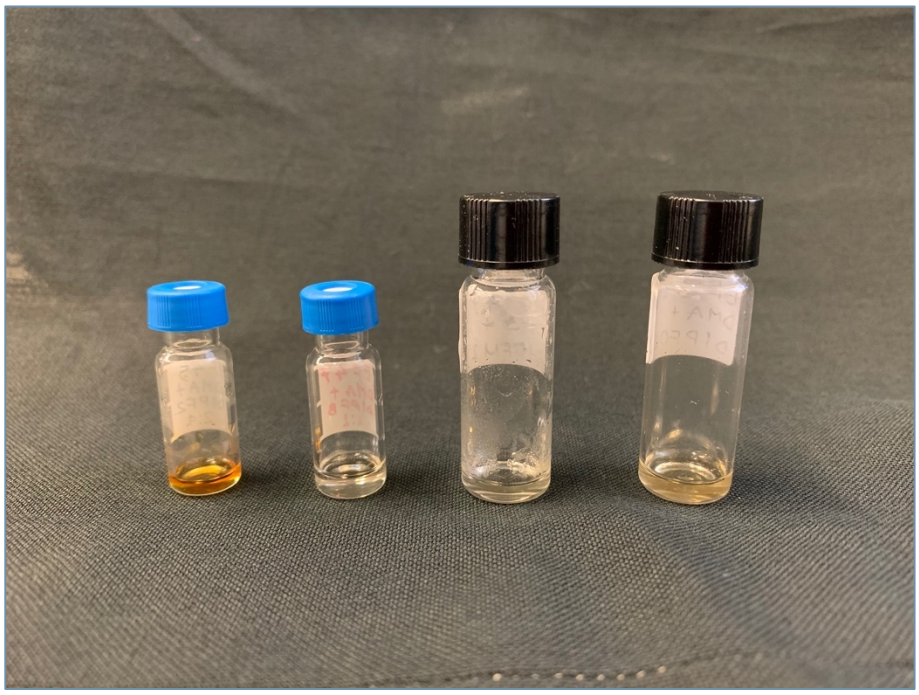

Figure 3.1: Liquid DMA/DIPFAs 2:1 complexes. From left to right: DMA/DIPF2, DMA/DIPF4, DMA/DIPF6, DMA/DIPF8.

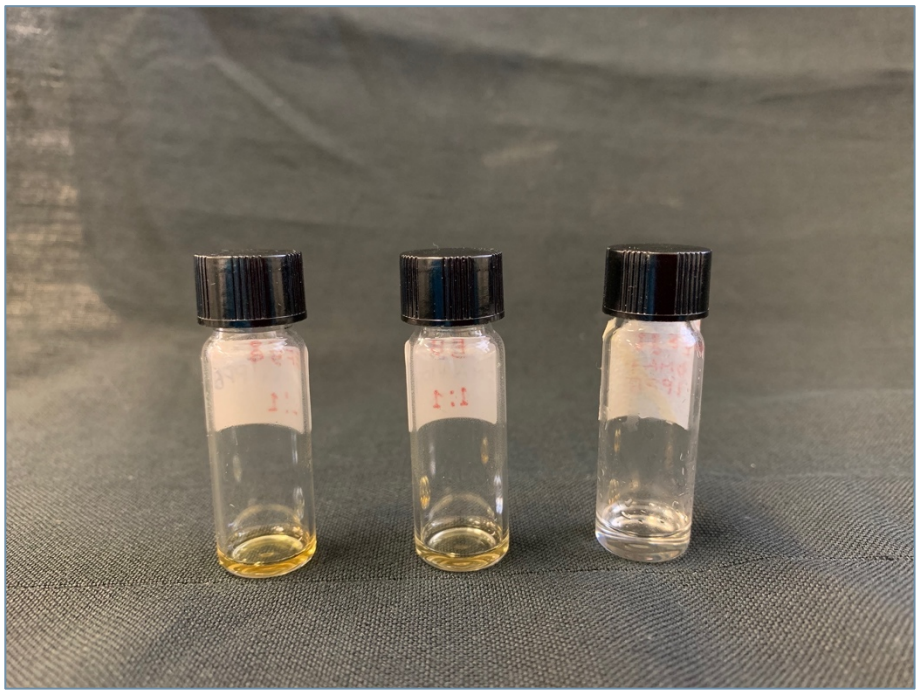

Figure 3.2: Liquid DMA/IPFAs 1:1 complexes. From left to right: DMA/IPF6, DMA/IPF8, DMA/IPFB.

Figure 3.3: Products of slow solvent evaporation co-crystallization of DMA/DITFB 2:1 (left) and DMA/IPFD 1:1 (right).

3.1.1. Differential Scanning Calorimetry

DSC analysis was able to give an indication on the stoichiometry of the complexes. The DSC of the DMA/DITFB, DMA/IPFD and DMA/DIPF2 in particular (Fig. 3.4-3.6) show that the complexes with 1 equivalent of iodine atoms per carbonyl have new melting and crystallization peaks, while the melting points of the pure compounds are absent. The samples with 2 equivalents instead show both new melting and crystallization peaks but also the melting peaks of non-bonded iodoperfluorocarbons, at slightly lower temperatures due to melting point depression caused by the impurities. This suggests that the carbonyl of DMA behave as a monodentate halogen bond acceptor.

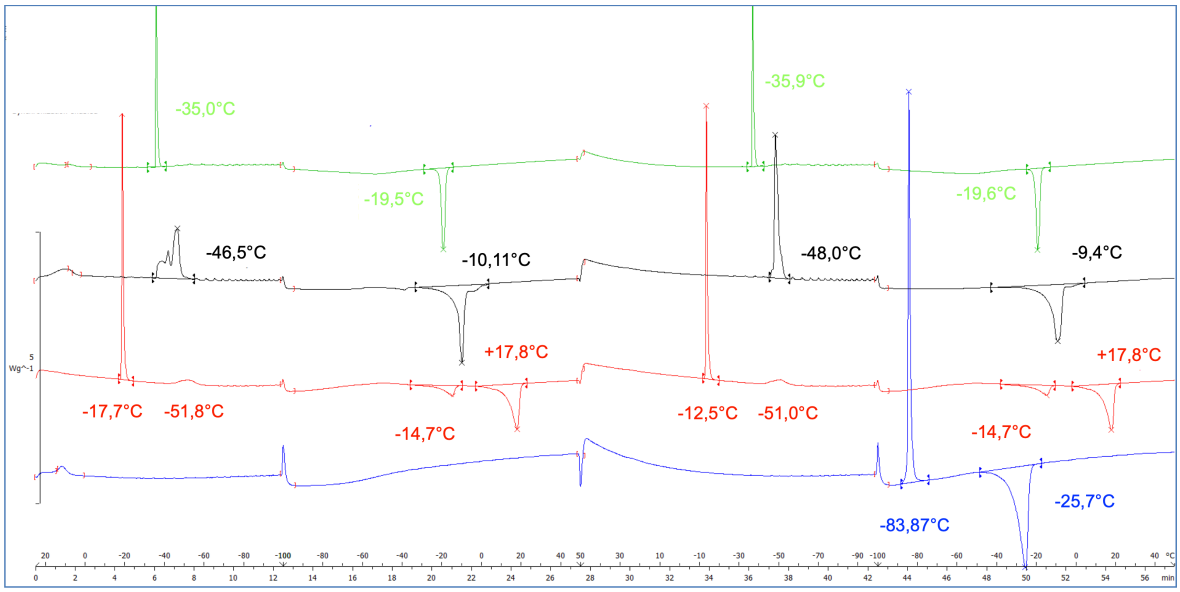

Figure 3.4: Comparison of the DSC analyses of pure DIPF2 (green), DMA/DIPF2 2:1 (black), DMA/DIPF2 1:1 (red) and pure DMA (blue). Method: +25/-100°C, -100/+50°C, +50/-100°C, -100/+50°C, heating and cooling rate 10°C/min.

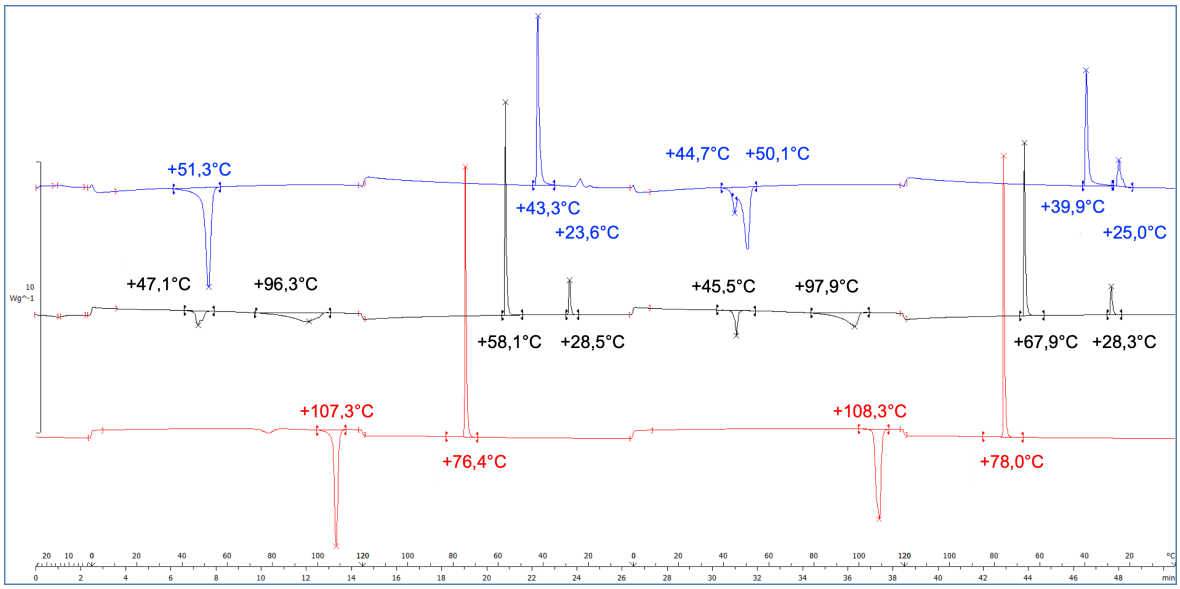

Figure 3.5: Comparison of the DSC analyses of DMA/DITFB 2:1 (blue), DMA/DITFB 1:1 (black), pure DITFB (red). Method: 0/+120°C, +120/0°C, 0/+120°C, +120/0°C, heating and cooling rate 10°C/min.

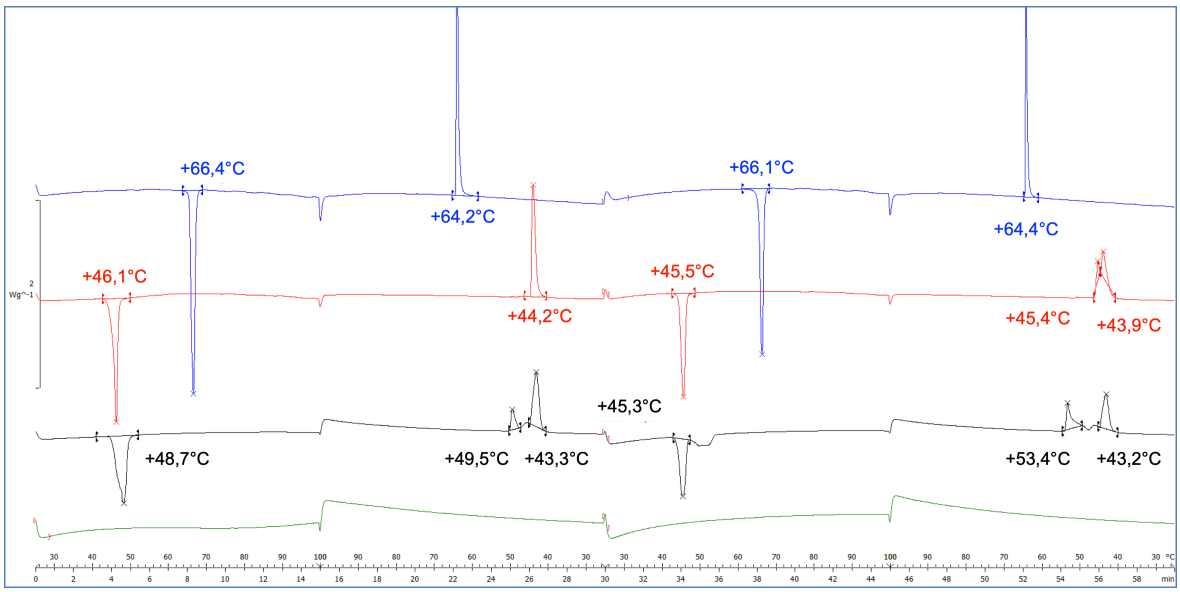

Figure 3.6: Comparison of the DSC analyses of pure IPF10 (blue), DMA/IPF10 1:1 (red), DMA/IPF10 2:1 (black) and pure DMA (green). Method: +25/+100°C, +100/+25°C, +25/+100°C, +100/+25°C, heating and cooling rate 5°C/min.

DSC was carried out also on the samples with the hydrogen bond donors: N,N-dimethylacrylamide/phenol, N,N-dimethylacrylamide/hydroquinone and N,N-

dimethylacrylamide/ethylene glycol. In each case, no fusion or crystallization peaks could be observed, as opposed to the corresponding halogen-bonded complexes with, respectively, iodopentafluorobenzene, 1,4-diiodotetrafluorobenzene, and 1,2-diiodotetrafluoroethane, which, during the same cooling and heating cycles, were able to crystallize.

3.1.2. FTIR Spectroscopy

IR spectra were collected for all the samples. As summarized in table 3.1, in each sample the peak associated to the C=O stretching resulted red-shifted, while the C—N stretching resulted blue-shifted, results compatible to what was observed in studies of the interaction between dimethylacetamide and iodine, and that confirm that the complex is formed with the oxygen of the carbonyl [52]. The expected shifts of the C—F stretching modes were also detected in the 1200-1000 cm^{-1} region.

The larger shifts were found for the DMA/DITFB co-crystals, and the complexes with diiodoperfluorocarbons showed smaller shifts of the C=O the longer the chain.

Table 3.1: ATR-FTIR principal shifts of DMA/DIPFA complexes.

Sample	$\tilde{\nu}$ C=O (cm^{-1})	$\delta\tilde{\nu}$ C=O (cm^{-1})	$\tilde{\nu}$ C–N (cm^{-1})	$\delta\tilde{\nu}$ C–N (cm^{-1})
Pure DMA	1647,47	-	1417,46	-
DMA/DITFB - 2 : 1	1639,88	-7,59	1419,93	2,47
DMA/DIPF2 - 2 : 1	1643,72	-3,75	1418,95	1,49
DMA/DIPF4 - 2 : 1	1644,05	-3,42	1419,82	2,36
DMA/DIPF6 - 2 : 1	1644,66	-2,81	1420,11	2,65
DMA/DIPF8 - 2 : 1	1644,79	-2,68	1420,52	3,06
DMA/DITFB - 1 : 1	1642,15	-5,32	1428,96	11,5
DMA/DIPF2 - 1 : 1	1643,18	-4,29	1419,62	2,16
DMA/DIPF4 - 1 : 1	1643,87	-3,6	1420,79	3,33
DMA/DIPF6 - 1 : 1	1643,96	-3,51	1421,26	3,8
DMA/DIPF8 - 1 : 1	1644,79	-2,68	1421,44	3,98

Considering the complexes with the monoiodoperfluorocarbons, the same shifts of the DMA can be observed, though they are of smaller entity with respect to the diiodoperfluoroalkanes, suggesting that the ditopic molecules are more efficient in the formation of the complex. No trend related to the length of the perfluorocarbon chain seems to emerge (table 3.2).

Table 3.2: ATR-FTIR principal shifts of DMA/IPFA complexes.

Sample	$\tilde{\nu}$ C=O (cm^{-1})	$\delta\tilde{\nu}$ C=O (cm^{-1})	$\tilde{\nu}$ C–N (cm^{-1})	$\delta\tilde{\nu}$ C–N (cm^{-1})
Pure DMA	1647,47	-	1417,46	-
DMA/IPFB - 1:1	1645,48	-1,99	1419,49	2,03
DMA/IPF6 - 1:1	1646,69	-0,78	1420,94	3,48
DMA/IPF8 - 1:1	1647,35	-0,12	1421,09	3,63
DMA/IPF10 - 1:1	1646,67	-0,8	1421,46	4,00
DMA/IPF6 - 1:2	1646,71	-0,76	1421,42	3,96
DMA/IPF8 - 1:2	1647,07	-0,40	1421,38	3,92
DMA/IPF10 - 1:2	1646,56	-0,91	1421,47	4,01

The samples with HB donors showed the same shifts of the DMA, confirming that the hydrogen-bonded complexes have also formed with the oxygen of the carbonyl.

Table 3.3: ATR-FTIR principal shifts of DMA/HB donor complexes. In parenthesis the value of the peaks for pure DMA are given.

Sample	$\tilde{\nu}$ C=O (cm^{-1})	$\delta\tilde{\nu}$ C=O (cm^{-1})	$\tilde{\nu}$ C–N (cm^{-1})	$\delta\tilde{\nu}$ C–N (cm^{-1})
Pure DMA	1647,47	-	1417,46	-
DMA/PH	1643,65	-3,82	1421,54	4,08
DMA/HQ	1643,14	-4,33	1421,53	4,07
DMA/EG	1644,92	-2,55	1419,89	2,43

3.1.3. Nuclear Magnetic Resonance Spectroscopy

NMR spectroscopy carried out on the liquid complexes of DMA was able to further confirm the occurrence of halogen bonding in the samples through shifts of the signals of the CF_2–I group. Considering for example the ^{19}F spectrum of DMA/DIPF2 (Fig. 3.7), the signal observed for DIPF2 in n-pentane falls at -52,48 ppm, while the complex has it at -56,82 ppm. Looking at all the samples, the changes in chemical shift of the peaks of the fluorine atoms close to iodine were between 4,34 and 6,11 ppm, with respect to solutions of only the XB donors in n-pentane (table 3.4). Comparing these values to that found for the pyridine/DIPF2 interaction of 7,32 ppm [53], it is confirmed that, while still able to form the interaction, carbonyl is not as good an XB acceptor as pyridine.

Table 3.4: Observed chemical shifts of the fluorine atoms close to iodine in the liquid DMA complexes.

Sample	δ -CF_2- in n-pentane (ppm)	δ -CF_2- in DMA (ppm)	$\Delta\delta$ -CF_2- (ppm)
DMA/DIPF2	-52,48	-56,82	4,34
DMA/DIPF4	-58,16	-63,66	5,5
DMA/DIPF6	-58,4	-64,03	5,63
DMA/DIPF8	-58,17	-64,28	6,11
DMA/IPF6	-58,84	-64,66	5,82
DMA/IPF8	-58,97	-64,13/-64,93	5,16/5,96

It is important to note that, as seen for example for the DMA/DIPF8 complex (Fig. 3.8), the chemical shifts observed for the fluorine atoms farther from iodine are much smaller if not completely absent, proof that the large shift observed is caused by the formation of the halogen bond and not by dilution effects.

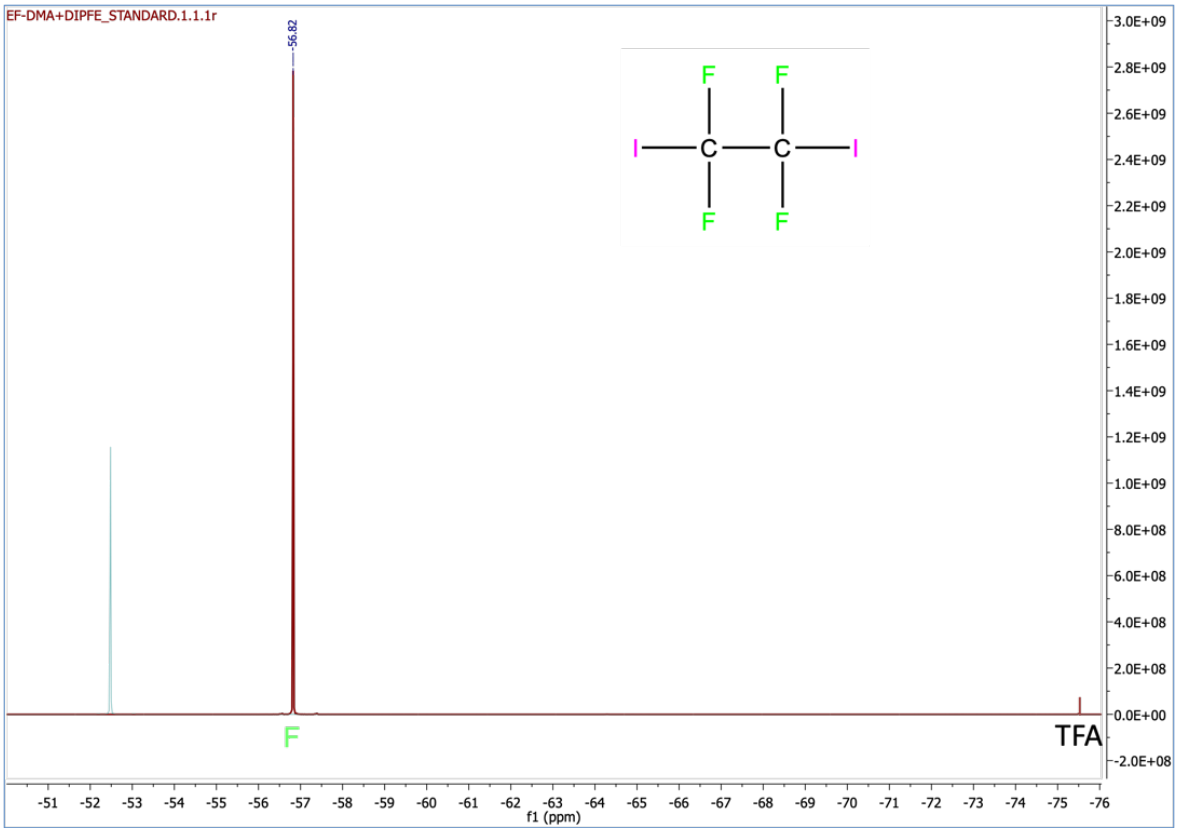

Figure 3.7: ^{19}F-NMR spectrum of DMA/DIPF2 complex (red line) compared to the spectrum of DIPF2 in n-pentane (light blue). The peak of TFA was fixed at 75,5 ppm as reference.

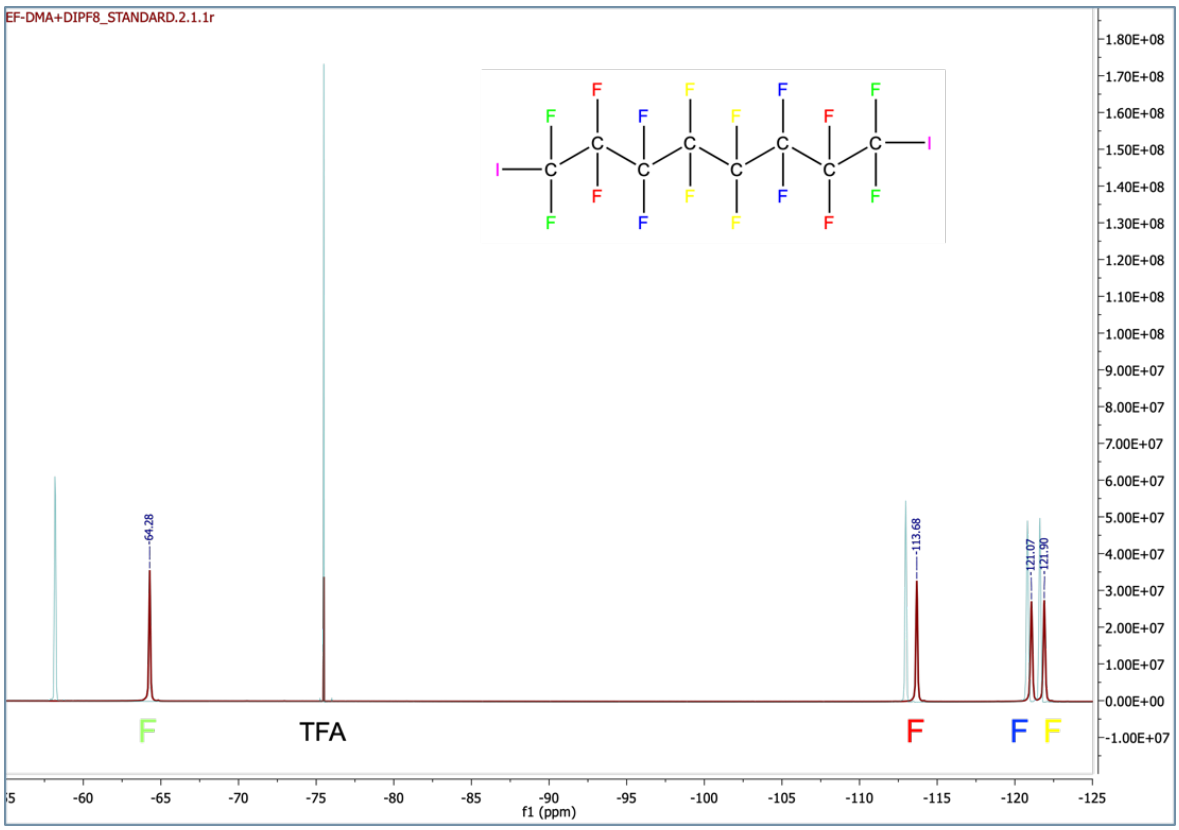

Figure 3.8: ^{19}F-NMR spectrum of DMA/DIPF8 complex (red line) compared to the spectrum of DIPF8 in n-pentane (light blue). The peak of TFA was fixed at 75,5 ppm as reference.

Regarding the complex with iodopentafluorobenzene (figure 3.9), the observed shifts are smaller, but the fact that the larger shift is observed for the fluorine atom in para position suggests that this might be due to a charge redistribution over the whole ring.

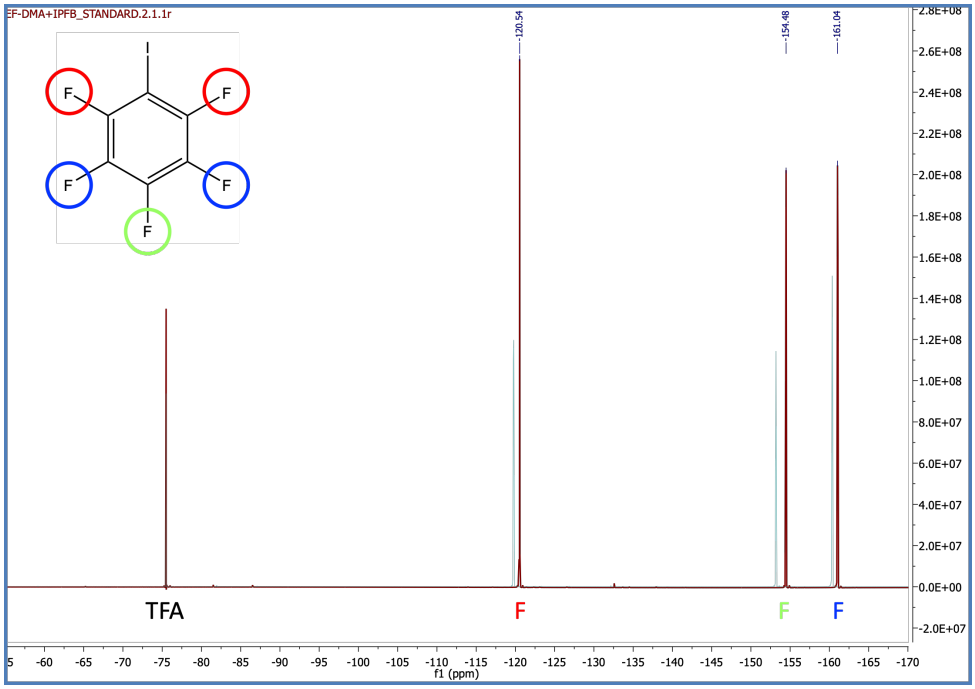

Figure 3.9: ^{19}F-NMR spectrum of the DMA/IPFB complex.

The NMR spectroscopies carried on the solid samples N,N-dimethylacrylamide/1-iodoperfluorodecane and N,N-dimethylacrylamide/1,4-diiodotetrafluorobenzene, being in solution with an interacting solvent like chloroform, showed small changes in chemical shifts, 0,10 ppm in the case of the DMA/IPF10 sample and 0,22 ppm in the case of DMA/DITFB.

3.2. N,N-Dimethylacrylamide Ternary Samples

The samples N,N-dimethylacrylamide/phenol/iodopentafluorobenzene (DMA/PH/IPFB) and N,N-dimethylacrylamide/ethylene glycol/1,2-diiodotetrafluoroethane (DMA/EG/DIPF2) did not show any formation of precipitate and were liquid at room temperature.

The N,N-dimethylacrylamide/hydroquinone/1,4-diiodotetrafluorobenzene (DMA/HQ/DITFB) sample instead showed formation of elongated crystals, similar to those obtained with DMA/DITFB, inside a red liquid phase, similar to the one observed with DMA/HQ.

3.2.1. FTIR Spectroscopy

FTIR spectra of each of the ternary samples showed the expected shifts of the C=O stretching and the C-N stretching of the DMA, with a particularly strong red shift of 11 cm-1 for the carbonyl in the DMA/PH/IPFB sample. It was also possible to observe peak shifts for the other two compounds present, the HB donor, and the XB donor. Analysis of the crystals found in DMA/HQ/DITFB showed that they consisted of the DMA/DITFB binary complex.

3.2.2. Differential Scanning Calorimetry

Through DSC of these ternary samples, it was possible to observe the peaks associated to the binary halogen-bonded complexes, but also the presence of small quantities of non-bonded perfluorocarbons. Considering what was reported for IR spectroscopy it is possible to advance the hypothesis that the DMA/XB complex has formed, and while it is possible that also the DMA/HB one is present, it can be

concluded that the ternary complex with DMA as both XB and HB acceptor has not formed.

3.3. Poly(N,N-dimethylacrylamide) Samples

The samples obtained through isothermal solvent evaporation showed different results depending on the IPFC used. PDMA/IPF6 resulted in a slightly yellow film, malleable and adherent to the walls of the vial. The PDMA/IPF8 sample instead consisted of a sticky paste. The samples of PDMA/IPF10 and PDMA/IPF12 both formed a slightly sticky powder. Finally, the PDMA/DITFB one formed a compact film strongly adherent to the walls of the vial.

In the case of the PDMA/IPF10 sample obtained through melting the mixture had assumed a yellow/orange tint, and IR spectroscopy showed smaller shifts with respect to the samples prepared with the other methods. This is probably due to the degradation of IPF10 due to the high temperature, with loss of iodine. Similar results were observed with IPF12 and DITFB, so it can be concluded that this method is not suitable for the self-assembly of PDMA with iodoperfluorocarbons.

3.3.1. FTIR Spectroscopy

IR analysis was performed on all the samples with XB donors and on the one with 3-pentadecylphenol.

Pure PDMA was dried before the analysis by heating it at 100°C and under vacuum for 30 minutes.

Comparison of the IR spectra of the PDMA/IPF10 samples obtained with different methods showed larger shifts of the C=O stretching with slow isothermal solvent evaporation, suggesting that better complexation is achieved with this method.

The shift reported in (table 3.5) were observed; regarding the signal of the carbonyl stretching, in the article by Faber et al. [46] the peak is reported at 1642 cm^{-1}, while the value obtained with PDMA/PDP was similar to what was measured, so residual amounts of water were probably still present in the analysed polymer, and the actual shifts of the samples are larger than what indicated in the table.

In the PDMA/IPF6 sample no signals of the IPF6 could be detected, meaning that in the slow solvent evaporation process used the volatile iodoperfluorocarbon evaporated almost completely before formation of the complex.

Table 3.5: C=O stretching peaks shifts observed in the PDMA complexes.

Sample	$\tilde{\nu}$ C=O (cm^{-1})	$\delta\tilde{\nu}$ C=O (cm^{-1})
Pure PDMA	1627,05	-
PDMA/IPF6	1616,10	-10,95
PDMA/IPF8	1613,85	-13,20
PDMA/IPF10	1614,80	-12,25
PDMA/DITFB	1617,86	-9,19
PDMA/DIPF8	1623,59	-3,46
PDMA/PDP	1618,50	-8,55

Some of the samples were also analysed in the far range, and for the PDMA/DITFB sample a red-shift of about 4 cm-1 of the C-I was observed (Fig 3.10).

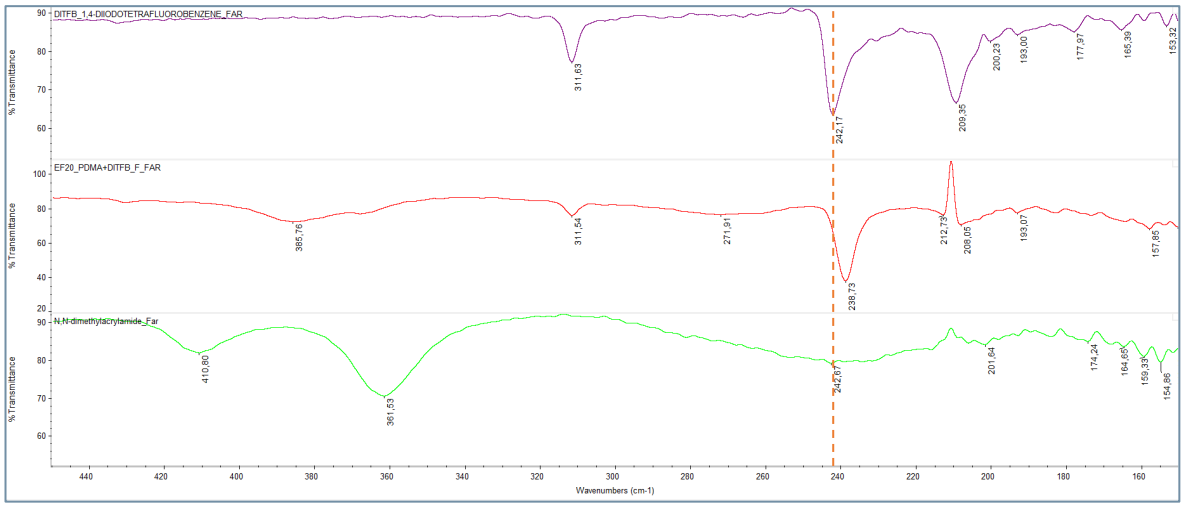

Figure 3.10: IR spectrum comparison in the far range of pure DITFB (purple), PDMA/DITFB (red), and pure DMA (green). The observed C-I shift has been highlighted.

3.3.2. Thermogravimetric Analysis

TGA was performed on all the PDMA binary complexes, but it was useful to determine the formation of a complex only for the diiodoperfluorocarbons (figure 3.11). One common feature of all thermograms though was the absence of weight loss around 100°C associated to water evaporation: upon formation of the halogen bond the absorbed water is expelled, meaning the halogen bond is able to prevail on hydrogen bond.

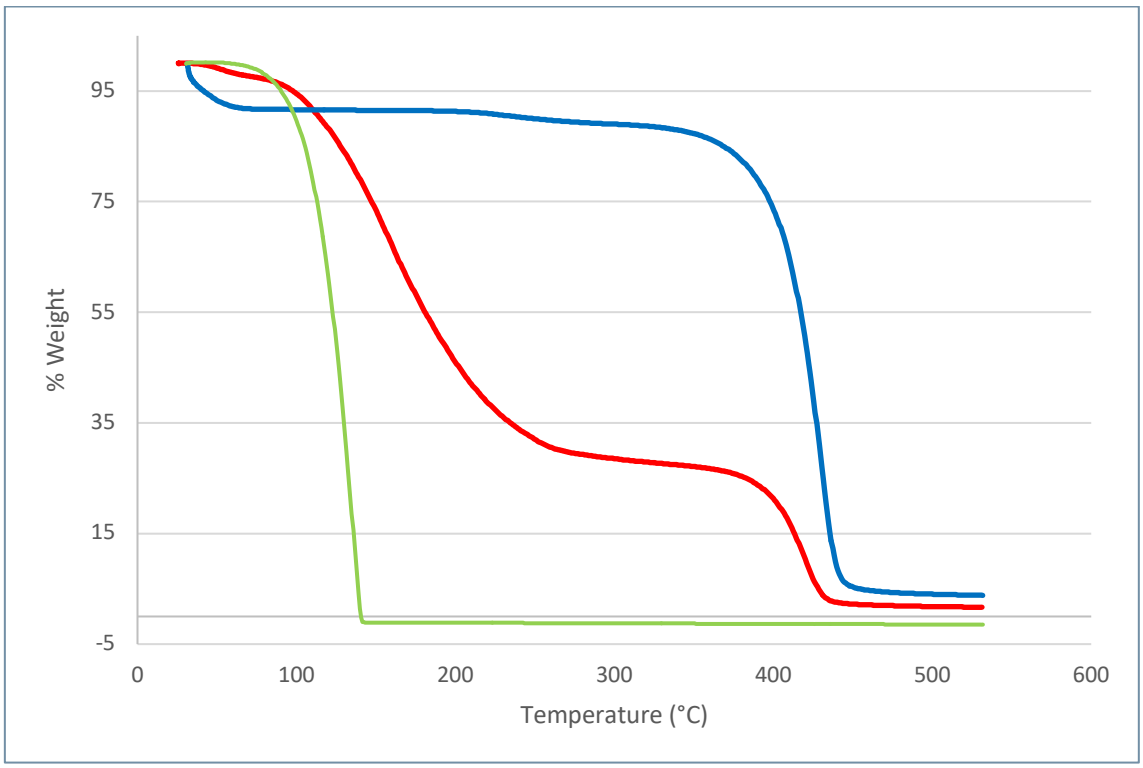

Figure 3.11: TGA of the PDMA/DITFB sample obtained through fast crystallization. The different trend in the curve of PDMA/DITFB (red line) with respect to pure DITFB (green line), suggest partial complexation of the iodoperfluorocarbon. The curve of pure PDMA is also shown (blue line)

3.3.3. Differential Scanning Calorimetry

DSC was performed on the PDMA/IPF8, PDMA/IPF10 and PDMA/DITFB samples, heating from 0 to 120°C and cooling from 120 to 0°C, at 10°C/min, for two runs. In the case of PDMA/IPF8 no fusion or crystallization peaks could be detected, compatible with the paste-like consistency observed, and the peaks of pure IPF8 were not detected. In the curve of PDMA/IPF10 a fusion peak was observed at 64,98°C, that is also present in the second run at 63,68°C, although smaller; the melting point of pure IPF10 is around 66°C, so it is difficult to conclude that what is observed is the melting peak of the complex. Regarding PDMA/DITFB, a small fusion peak at 48,5°C was present in in the first run, while the fusion peak of pure DITFB around 107°C was absent; the lower melting point is consistent with what

was observed in the model with DMA and confirms the formation of the supramolecular complex.

4 Conclusions

The preparation and characterization of the model system with N,N-dimethylacrylamide and various halogen bond donors has been performed with positive results.

Through differential scanning calorimetry the appearance of new fusion and crystallization peaks, particularly evident in the DMA/DIPF2 liquid complex and in the DMA/IPF10 and DMA/DITFB solid complexes, were detected, first evidence of the formation of a supramolecular interaction between the monomer and the halogen bond donor. Through these analyses it was also possible to determine that the oxygen of the carbonyl acts as a monodentate XB acceptor site.

The occurrence of halogen bond interaction was confirmed with IR spectroscopy, where the expected shifts of C=O, C–N and C–F signals were observed in all the samples, compatible with the formation of an O···I bond. The larger shifts observed in the complexes with ditopic XB donors with respect to the monotopic ones suggest that stronger complexation is achieved with the former.

Through 19F-NMR of the pure liquid complexes it was possible to confirm the formation of the interaction through the large, up-field, shifts of the signal of the fluorine atoms close to the iodine atom involved in the XB. Small shifts were also observed in the spectra of the solid DMA/IPF10 and DMA/DITFB complexes.

The first studies on the ternary complexes seem instead to show that C=O is not able to act as a site for orthogonal XB and HB, since, while IR spectroscopy shows

peak shifts for all the components, the fusion and crystallization peaks observed with DSC indicate that only the binary halogen-bonded and hydrogen-bonded complexes have formed.

The occurrence of the interaction has been proved, but the model system of N,N-dimethylacrylamide with the iodoperfluorocarbons can be explored further: through NMR titration the equilibrium constants of the various complex formations can be determined, and cryo-crystallization can be attempted on the DMA/DIPF2 liquid complex, with the hope to determine a new crystal structure. Following the article by Le, Wang and Goto [40], study on the polymerization of DMA with the different iodoperfluorocarbons is an interesting perspective. Since complexes both liquid and solid have been obtained, photopolymerization experiments both in solution and in solid phase can be attempted, to investigate the effect of the length of the perfluorocarbon chain and of the number of XB donor sites on molecular weight, polydispersity, tacticity, and structure of the final polymer.

The first experiments performed on poly(N,N-dimethylacrylamide) were able to confirm the formation of the interaction with all the iodoperfluorocarbons through FTIR spectroscopy, and for the PDMA/DITFB complex further proofs were obtained with TGA and DSC.

To conclude, this master thesis work has shown, first through characterization of the model system with DMA and then with the first studies on the polymer, that PDMA can successfully form halogen-bonded supramolecular complexes with a variety of iodoperfluorocarbons. To the best of my knowledge no reports on the self-assembly of poly(N,N-dimethylacrylamide) with halogen bond are present in literature, so the results drawn from this work open new possibilities in the design of halogen-bonded supramolecular polymer systems.

Bibliography

[1] O. Ikkala and G. Ten Brinke, "Functional materials based on self-assembly of polymeric supramolecules," *Science (80-.).*, vol. 295, no. 5564, pp. 2407–2409, 2002, doi: 10.1126/science.1067794.

[2] G. Krausch and R. Magerle, "Nanostructured thin films via self-assembly of block copolymers," *Adv. Mater.*, vol. 14, no. 21, pp. 1579–1583, 2002, doi: 10.1002/1521-4095(20021104)14:21<1579::AID-ADMA1579>3.0.CO;2-6.

[3] B. Copolymers, F. H. Schacher, P. A. Rupar, and I. Manners, "Functional Block Copolymers : Nanostructured Materials with Emerging Applications Angewandte," pp. 7898–7921, 2012, doi: 10.1002/anie.201200310.

[4] M. Robertson, Q. Zhou, C. Ye, and Z. Qiang, "Developing Anisotropy in Self-Assembled Block Copolymers : Methods , Properties , and Applications," vol. 2100300, pp. 1–32, 2021, doi: 10.1002/marc.202100300.

[5] C. T. Black, "Polymer self-assembly as a novel extension to optical lithography," *ACS Nano*, vol. 1, no. 3, pp. 147–150, 2007, doi: 10.1021/nn7002663.

[6] K. H. Lo, M. C. Chen, R. M. Ho, and H. W. Sung, "Pore-filling nanoporous templates from degradable block copolymers for nanoscale drug delivery,"

ACS Nano, vol. 3, no. 9, pp. 2660–2666, 2009, doi: 10.1021/nn900299z.

[7] A. Sidorenko, I. Tokarev, S. Minko, and M. Stamm, "Ordered Reactive Nanomembranes / Nanotemplates from Thin Films of Block Copolymer Supramolecular Assembly," no. 11, pp. 12211–12216, 2003.

[8] A. Blanazs, S. P. Armes, and A. J. Ryan, "Self-Assembled Block Copolymer Aggregates : From Micelles to Vesicles and their Biological Applications," pp. 267–277, 2009, doi: 10.1002/marc.200800713.

[9] N. Nishiyama, Y. Bae, K. Miyata, S. Fukushima, and K. Kataoka, "Smart polymeric micelles for gene and drug delivery," pp. 21–26, 2005, doi: 10.1016/j.ddtec.2005.05.007.

[10] B. Rybtchinski, "Adaptive supramolecular nanomaterials based on strong noncovalent interactions," *ACS Nano*, vol. 5, no. 9, pp. 6791–6818, 2011, doi: 10.1021/nn2025397.

[11] J. M. Pollino and M. Weck, "Non-covalent side-chain polymers: Design principles, functionalization strategies, and perspectives," *Chem. Soc. Rev.*, vol. 34, no. 3, pp. 193–207, 2005, doi: 10.1039/b311285n.

[12] D. B. Amabilino, D. K. Smith, and J. W. Steed, "Supramolecular materials," *Chem. Soc. Rev.*, vol. 46, no. 9, pp. 2404–2420, 2017, doi: 10.1039/c7cs00163k.

[13] B. J. Ruokolainen and G. Brinke, "Supramolecular Polymeric Materials with Hierarchical Structure-Within-Structure Morphologies **," pp. 777–780, 1999.

[14] W. J. Mullin and S. W. T. Iii, "Optimizing the self-assembly of conjugated polymers and small molecules through structurally programmed non-covalent control," no. April, pp. 1643–1663, 2021, doi: 10.1002/pol.20210290.

[15] H. L. D. Copolymer, B. C. Osuji, C. Chao, I. Bita, C. K. Ober, and E. L. Thomas,

"Temperature-Dependent Photonic Bandgap in a Self-Assembled," no. 11, pp. 753–758, 2002.

[16] S. Valkama *et al.*, "Self-assembled polymeric solid fi lms with temperature-induced large and reversible photonic-bandgap switching," vol. 3, no. December, pp. 1–5, 2004, doi: 10.1038/nmat1254.

[17] G. T. E. N. Brinke and O. Ikkala, "Smart Materials Based on," pp. 219–230, 2004, doi: 10.1002/tcr.20018.

[18] G. Cavallo *et al.*, "The halogen bond," *Chem. Rev.*, vol. 116, no. 4, pp. 2478–2601, 2016, doi: 10.1021/acs.chemrev.5b00484.

[19] R. Kampes, S. Zechel, M. D. Hager, and U. S. Schubert, "Halogen bonding in polymer science: Towards new smart materials," *Chem. Sci.*, vol. 12, no. 27, pp. 9275–9286, 2021, doi: 10.1039/d1sc02608a.

[20] P. Metrangolo, "IUPAC definition of the halogen bond," *Acta Crystallogr. Sect. A Found. Adv.*, vol. 73, no. a2, pp. C309–C309, 2017, doi: 10.1107/s2053273317092646.

[21] P. Metrangolo, F. Meyer, T. Pilati, G. Resnati, and G. Terraneo, "Halogen bonding in supramolecular chemistry," *Angew. Chemie - Int. Ed.*, vol. 47, no. 33, pp. 6114–6127, 2008, doi: 10.1002/anie.200800128.

[22] C. Präsang, A. C. Whitwood, and D. W. Bruce, "Halogen-bonded cocrystals of 4-(N,N-dimethylamino)pyridine with fluorinated iodobenzenes," *Cryst. Growth Des.*, vol. 9, no. 12, pp. 5319–5326, 2009, doi: 10.1021/cg900823d.

[23] Y. Lu, Y. Wang, and W. Zhu, "Nonbonding interactions of organic halogens in biological systems: Implications for drug discovery and biomolecular design," *Phys. Chem. Chem. Phys.*, vol. 12, no. 18, pp. 4543–4551, 2010, doi:

10.1039/b926326h.

[24] J. Martí-Rujas *et al.*, "Hydrogen and halogen bonding drive the orthogonal self-assembly of an organic framework possessing 2D channels," *Chem. Commun.*, vol. 48, no. 66, pp. 8207–8209, 2012, doi: 10.1039/c2cc33682k.

[25] V. Vasylyeva, S. K. Nayak, G. Terraneo, G. Cavallo, P. Metrangolo, and G. Resnati, "Orthogonal halogen and hydrogen bonds involving a peptide bond model," *CrystEngComm*, vol. 16, no. 35, pp. 8102–8105, 2014, doi: 10.1039/c4ce01514b.

[26] G. R. Desiraju, "Crystal engineering: From molecule to crystal," *J. Am. Chem. Soc.*, vol. 135, no. 27, pp. 9952–9967, 2013, doi: 10.1021/ja403264c.

[27] H. L. Nguyen, P. N. Horton, M. B. Hursthouse, A. C. Legon, and D. W. Bruce, "Halogen Bonding: A New Interaction for Liquid Crystal Formation," *J. Am. Chem. Soc.*, vol. 126, no. 1, pp. 16–17, 2004, doi: 10.1021/ja036994l.

[28] P. Metrangolo, C. Präsang, G. Resnati, R. Liantonio, A. C. Whitwood, and D. W. Bruce, "Fluorinated liquid crystals formed by halogen bonding," *Chem. Commun.*, no. 31, pp. 3290–3292, 2006, doi: 10.1039/b605101d.

[29] A. R. Hirst, B. Escuder, J. F. Miravet, and D. K. Smith, "High-tech applications of self-assembling supramolecular nanostructured gel-phase materials: From regenerative medicine to electronic devices," *Angew. Chemie - Int. Ed.*, vol. 47, no. 42, pp. 8002–8018, 2008, doi: 10.1002/anie.200800022.

[30] L. Meazza, J. A. Foster, K. Fucke, P. Metrangolo, G. Resnati, and J. W. Steed, "Halogen-bonding-triggered supramolecular gel formation," *Nat. Chem.*, vol. 5, no. 1, pp. 42–47, 2013, doi: 10.1038/nchem.1496.

[31] S. Varghese and S. Das, "Role of molecular packing in determining solid-state

optical properties of π-conjugated materials," *J. Phys. Chem. Lett.*, vol. 2, no. 8, pp. 863–873, 2011, doi: 10.1021/jz200099p.

[32] G. M. Day *et al.*, "A Cocrystal Strategy to Tune the Luminescent Properties of Stilbene- Type Organic Solid-State Materials **," pp. 12483–12486, 2011, doi: 10.1002/anie.201106391.

[33] A. Priimagi *et al.*, "Photoalignment and surface-relief-grating formation are efficiently combined in low-molecular-weight halogen-bonded complexes," *Adv. Mater.*, vol. 24, no. 44, pp. 345–352, 2012, doi: 10.1002/adma.201204060.

[34] R. Bertani *et al.*, "Supramolecular route to fluorinated coatings: Self-assembly between poly(4-vinylpyridines) and haloperfluorocarbons," *Adv. Mater.*, vol. 14, no. 17, pp. 1197–1201, 2002, doi: 10.1002/1521-4095(20020903)14:17<1197::AID-ADMA1197>3.0.CO;2-V.

[35] R. Milani *et al.*, "Hierarchical Self-Assembly of Halogen-Bonded Block Copolymer Complexes into Upright Cylindrical Domains," *Chem*, vol. 2, no. 3, pp. 417–426, 2017, doi: 10.1016/j.chempr.2017.02.003.

[36] N. Houbenov *et al.*, "Halogen-bonded mesogens direct polymer self-assemblies up to millimetre length scale," *Nat. Commun.*, vol. 5, no. May, pp. 1–8, 2014, doi: 10.1038/ncomms5043.

[37] F. Wang, N. Ma, Q. Chen, W. Wang, and L. Wang, "Halogen bonding as a new driving force for layer-by-layer assembly," *Langmuir*, vol. 23, no. 19, pp. 9540–9542, 2007, doi: 10.1021/la701969q.

[38] A. Vanderkooy and M. S. Taylor, "Solution-phase self-assembly of complementary halogen bonding polymers," *J. Am. Chem. Soc.*, vol. 137, no. 15, pp. 5080–5086, 2015, doi: 10.1021/jacs.5b00754.

[39] K. Hema, A. Ravi, C. Raju, J. R. Pathan, R. Rai, and K. M. Sureshan, "Topochemical polymerizations for the solid-state synthesis of organic polymers," *Chem. Soc. Rev.*, vol. 50, no. 6, pp. 4062–4099, 2021, doi: 10.1039/d0cs00840k.

[40] H. T. Le, C. G. Wang, and A. Goto, "Solid-Phase Radical Polymerization of Halogen-Bond-Based Crystals and Applications to Pre-Shaped Polymer Materials," *Angew. Chemie - Int. Ed.*, vol. 59, no. 24, pp. 9360–9364, 2020, doi: 10.1002/anie.202001544.

[41] A. Priimagi *et al.*, "Halogen bonding versus hydrogen bonding in driving self-assembly and performance of light-responsive supramolecular polymers," *Adv. Funct. Mater.*, vol. 22, no. 12, pp. 2572–2579, 2012, doi: 10.1002/adfm.201200135.

[42] F. Herbst, D. Döhler, P. Michael, and W. H. Binder, "Self-healing polymers via supramolecular forces," *Macromol. Rapid Commun.*, vol. 34, no. 3, pp. 203–220, 2013, doi: 10.1002/marc.201200675.

[43] R. Tepper *et al.*, "Polymeric Halogen-Bond-Based Donor Systems Showing Self-Healing Behavior in Thin Films," *Angew. Chemie - Int. Ed.*, vol. 56, no. 14, pp. 4047–4051, 2017, doi: 10.1002/anie.201610406.

[44] L. Song, D. Liang, Z. Chen, D. Fang, and B. Chu, "DNA sequencing by capillary electrophoresis using mixtures of polyacrylamide and poly(N,N-dimethylacrylamide)," *J. Chromatogr. A*, vol. 915, no. 1–2, pp. 231–239, 2001, doi: 10.1016/S0021-9673(01)00593-3.

[45] M. Gregori *et al.*, "Investigation of Functionalized Poly(N,N-dimethylacrylamide)-block-polystyrene Nanoparticles As Novel Drug Delivery System to Overcome the Blood-Brain Barrier in Vitro," *Macromol.*

Biosci., vol. 15, no. 12, pp. 1687–1697, 2015, doi: 10.1002/mabi.201500172.

[46] M. Faber *et al.*, "Hierarchical self-assembly in supramolecular double-comb diblock copolymer complexes," *Macromolecules*, vol. 46, no. 2, pp. 500–517, 2013, doi: 10.1021/ma302295v.

[47] F. C. Pigge, V. R. Vangala, and D. C. Swenson, "Relative importance of X … O L C vs . X … X halogen bonding as structural determinants in 4-halotriaroylbenzenes {," pp. 2123–2125, 2006, doi: 10.1039/b603110b.

[48] K. Boubekeur and B. Scho, "First molecular self-assembly of 1 , 4-diiodo-tetrafluoro-benzene and a ketone via (O / I) non-covalent halogen bonds," vol. 737, pp. 103–107, 2005, doi: 10.1016/j.molstruc.2004.10.008.

[49] J. D. Menczel, L. Judovits, R. B. Prime, H. E. Bair, M. Reading, and S. Swier, "Differential Scanning Calorimetry (DSC)," in *Thermal Analysis of Polymers: Fundamentals and Applications*, 2008.

[50] D. A. Skoog, F. J. Holler, and S. R. Crouch, *Principles of Insrtumental Analysis 7th Edition*, no. 3. 2018.

[51] N. Saadatkhah *et al.*, "Experimental methods in chemical engineering: Thermogravimetric analysis—TGA," *Canadian Journal of Chemical Engineering*, vol. 98, no. 1. 2020, doi: 10.1002/cjce.23673.

[52] C. . Schmulbach and R. S. Drago, "Molecular Addition Compounds of Iodine. III. An Infrared Investigation of the Interaction Between Dimethylacetamide and Iodine," vol. 713, no. 1954, pp. 4484–4487, 1960.

[53] M. T. Messina, P. Metrangolo, W. Panzeri, E. Ragg, and G. R. L, "Perfluorocarbon-Hydrocarbon Self-Assembly. Part 3. Liquid Phase Interactions between Perfluoroalkylhalides and Heteroatom Containing

Hydrocarbons," vol. 39, pp. 9069–9072, 1998.

List of Figures

List of Tables

List of Abbreviations

Abbreviation	Meaning
DIPF2	1,2-diiodoperfluoroethane
DIPF4	1,4-diiodoperfluorobutane
DIPF6	1,6-diiododoperfluorohexane
DIPF8	1,8-diiodoperfluorooctane
DIPFA	Diiodoperfluoroalkane
DITFB	1,4-diiodotetrafluorobenzene
DMA	N,N-Dimethylacrylamide
EG	Ethylene glycol
HQ	Hydroquinone
IPF6	1-iodoperfluorohexane
IPF8	1-iodoperfluorooctane
IPF10	1-iodoperfluorodecane
IPF12	1-iodoperfluorododecane
IPFA	Iodoperfluoroalkane
IPFB	Iodopentafluorobenzane
PDMA	Poly(N,N-dimethylacrylamide)
PH	Phenol

Acknowledgments

I would like to thank Professor Pierangelo Metrangolo for the opportunity to work on this master thesis project, Professor Gabriella Cavallo that has supervised me with much patience, and all the members of SBNLab for the help, insight and company shared in these months.